

Geographic Routing for Wireless Networks

A thesis presented

by

Brad Nelson Karp

to

The Division of Engineering and Applied Sciences

in partial fulfillment of the requirements

for the degree of

Doctor of Philosophy

in the subject of

Computer Science

Harvard University

Cambridge, Massachusetts

October 2000

©2000 Brad Nelson Karp
All rights reserved.

Geographic Routing for Wireless Networks

Distributed shortest-path routing protocols for wired networks either describe the entire topology of a network or provide a digest of the topology to every router. They continually update the state describing the topology at all routers as the topology changes to find correct routes for all destinations. Hence, to find routes robustly, they generate routing protocol message traffic proportional to the product of the number of routers in the network and the rate of topological change in the network. Current ad-hoc routing protocols, designed specifically for mobile, wireless networks, exhibit similar scaling properties. It is the reliance of these routing protocols on state concerning all links in the network, or all links on a path between a source and destination, that is responsible for their poor scaling.

We present Greedy Perimeter Stateless Routing (GPSR), a novel routing protocol for wireless datagram networks that uses the *positions* of routers and a packet's destination to make packet forwarding decisions. GPSR makes *greedy* forwarding decisions using only information about a router's immediate neighbors in the network topology. When a packet reaches a region where greedy forwarding is impossible, the algorithm recovers by routing around the *perimeter* of the region. By keeping state only about the local topology, GPSR scales better in per-router state than shortest-path and ad-hoc routing protocols as the number of network destinations increases. Under mobility's frequent topology changes, GPSR can use local topology information to find correct new routes quickly. We describe the GPSR protocol, and use extensive simulation of mobile wireless networks to compare its performance with that of Dynamic Source Routing. Our simulations demonstrate GPSR's

scalability on densely deployed wireless networks.

Contents

1	Introduction	1
1.1	Metrics for Evaluating Routing Scalability	3
1.2	Traditional Shortest-Path Algorithms	4
1.3	Ad-Hoc Routing Algorithms	5
1.4	Techniques for Routing Scalability	7
1.5	Applicability of Scalable Wireless Routing	8
1.6	Assumptions	10
1.7	Thesis Contents	11
2	Greedy Forwarding	13
2.1	Greedy Forwarding Rule	13
2.2	Beaconing Protocol	14
2.3	Advantages of Greedy Forwarding	17
2.4	Limits to Greedy Forwarding's Applicability: Voids	18
2.5	Simulations: The Role of Density	20
3	The Right-Hand Rule: Perimeters	24

3.1	The Right-Hand Rule	25
3.2	Perimeter Probing	28
3.2.1	Greedy Perimeter Probing (GPP) Algorithm	28
3.2.2	Simulation and Evaluation of GPP	30
3.2.3	Routing Failures in GPP	35
3.3	Planarized Graphs	39
3.4	GPSR: Combining Greedy and Planar Perimeters	44
3.5	Robustness and Efficiency on Mobile Networks	52
3.5.1	Use of MAC-Layer Failure Feedback	53
3.5.2	Interface Queue Traversal	53
3.5.3	Promiscuous Use of the Network Interface	54
3.5.4	Planarization Triggers	55
4	Simulation Results and Evaluation	56
4.1	Simulation Environment	56
4.2	Packet Delivery Success Rate	61
4.3	Routing Protocol Overhead	62
4.4	Path Length	63
4.5	Effect of Network Diameter	66
4.6	Effect of Node Density	71
4.7	State per Router	79
5	Discussion and Future Work	81

5.1	GPSR's Properties	81
5.2	System Design for GPSR Networks	85
5.3	Future Work	87
6	Related Work	92
7	Conclusion	97

List of Figures

2.1	Greedy forwarding example. y is x 's closest neighbor to D	14
2.2	Greedy forwarding rule pseudocode.	15
2.3	Greedy forwarding failure.	19
2.4	Node x 's <i>void</i> with respect to destination D	19
2.5	Existing paths and greedy paths, 1500 m by 300 m region. 10–300 nodes, in increments of 5. Radio range is 250 m.	20
2.6	Existing paths and greedy paths, 670 m by 670 m region. 10–300 nodes, in increments of 5. Radio range is 250 m.	21
2.7	Existing paths and greedy paths, 3000 m by 600 m region. 10–300 nodes, in increments of 5. Radio range is 250 m.	21
2.8	Existing paths and greedy paths. 1340 m by 1340 m region. 10–300 nodes, in increments of 5. Radio range is 250 m.	22
3.1	The right-hand rule.	25
3.2	Right-hand rule forwarding pseudocode.	26
3.3	A network with crossing edges.	27

3.4	The GPP (Greedy Perimeter Probing) algorithm: PERI-CLOSER-LOOKUP and GPP-FORWARD.	31
3.5	Mixed forwarding.	32
3.6	Percentage of all n^2 routes <i>not</i> found, GPP.	33
3.7	State per router, GPP vs. Distance-Vector.	34
3.8	Failure of the no-crossing rule.	37
3.9	Perimeter with no closer node, but with an edge containing a closer point.	37
3.10	The RNG graph.	40
3.11	The GG graph.	42
3.12	Full, GG subset, and RNG subset radio graphs.	43
3.13	Perimeter forwarding example.	46
3.14	Pseudocode for GPSR.	49
4.1	Packet Delivery Success Rate. GPSR with varying beacon intervals, B , compared with DSR. 50 nodes.	62
4.2	Routing Protocol Overhead. Total routing protocol packets sent network- wide during the simulation for GPSR with varying beacon intervals, B , compared with DSR. 50 nodes.	64
4.3	Path length beyond optimal for GPSR's and DSR's successfully delivered packets. 50 nodes.	65
4.4	Packet Delivery Success Rate. For GPSR with $B = 1.5$ compared with DSR. 112 nodes.	69

4.5	Routing Protocol Overhead. Total routing protocol packets sent network-wide during the simulation for GPSR with $B = 1.5$ compared with DSR. 112 nodes.	70
4.6	Packet Delivery Success Rate. For GPSR with $B = 1.5$ compared with DSR. 200 nodes.	70
4.7	Routing Protocol Overhead. Total routing protocol packets sent network-wide during the simulation for GPSR with $B = 1.5$ compared with DSR. y axis log-scaled. 200 nodes.	71
4.8	Path length beyond optimal for GPSR's and DSR's successfully delivered packets. 112 nodes.	72
4.9	Path length beyond optimal for GPSR's and DSR's successfully delivered packets. 200 nodes.	73
4.10	Packet Delivery Success Rate. For GPSR with $B = 1.5$ compared with DSR. 50 nodes, sparse topology.	75
4.11	Routing Protocol Overhead. Total routing protocol packets sent network-wide during the simulation for GPSR with $B = 1.5$ compared with DSR. 50 nodes, sparse topology.	77
4.12	Path length beyond optimal for GPSR's and DSR's successfully delivered packets. 50 nodes, sparse topology.	78
4.13	Average state size stored, 200-node, pause-time-0 simulations, DSR vs. GPSR. Left: nodes stored; right: bytes stored.	80
5.1	An inner perimeter closing around a packet.	83

*There is nothing better for a man,
than that he should eat and drink,
and that he should make his soul
enjoy good in his labor.
Ecclesiastes, 2:24*

*And further, by these, my son, be admonished:
of making many books there is no end;
and much study is a weariness of the flesh.
Ecclesiastes, 12:12*

*Der Mann überlegt und fragt dann,
ob er also später werde eintreten dürfen.
“Es ist möglich,” sagt der Türhüter, “jetzt aber nicht.”*

...
*“Wenn es so dich lockt, versuche es doch,
trotz meines Verbotes hineinzugehn.
Merke aber: ich bin mächtig.
Und ich bin nur der unterste Türhüter.
Von Saal zu Saal ist stehn aber Türhüter,
einer mächtiger als der andere.
Schon den Anblick des dritten kann
nicht einmal ich mehr ertragen.”*
Franz Kafka, *Vor dem Gesetz*, in *Der Prozeß*

Acknowledgements

H. T. Kung, my thesis advisor, taught me the lesson I needed most to learn: that research requires a sometimes paradoxical combination of critical, truly long-term thinking when evaluating and directing one’s own work, with an inner confidence that one can, with sufficient dedication over time, contribute. Would that I could learn to duplicate his boundless energy. The high standards he has imparted to me will benefit my research efforts my whole life long.

Michael Mitzenmacher, my thesis committee member, made himself available for many chats, often precipitated by my dropping by his office unexpectedly, about the content and

presentation of this thesis. I always left these chats with a clearer understanding—and a more clearly and precisely written thesis—than I'd had when I arrived. Mike Smith, my other committee member, has unstintingly offered sound advice over the years. His calm, wisdom, and focus are a potent instance of advising by example.

I have been incredibly fortunate to have had labmates who are not merely stellar computer scientists—they are also wonderful friends. The hours of creative discussion, arguing, meals, and pure hilarity I've shared with Robert Morris, Dong Lin, Trevor Blackwell, and Koling Chang have been priceless, and seem entirely too few. May the Bonehed Consortium never fall!

I am especially grateful for the friendship of Robert Morris. Since our first year in lab, on the day I introduced myself to him, and to break the ice rendered into English the most shocking joke I'd heard just days before in France, I've enjoyed so many discussions that have shaped and enriched my view of systems and networks. His insight benefitted this thesis, as well.

Allison Mankin generously supported my research efforts for two years. But beyond that, the support she provided in the way of technical discussions, advice, and friendship were invaluable.

I profited immensely from my ten-month visit to ACIRI, ending in May 2000, during which I developed much of the latter part of this thesis. Mark Handley made my visit possible initially, and Scott Shenker gave me the chance to stay much longer thereafter. Dick Karp first suggested I investigate planar graphs, and this thesis benefitted generally from many discussions with Mark Handley, Scott Shenker, and the rest of ACIRI.

Chapter 1

Introduction

In networks comprised entirely of wireless stations, communication between source and destination nodes may require traversal of multiple hops, as radio ranges are limited. Traditional approaches to the *routing problem* of finding a sequence of hops between the originator of a packet and the packet's destination work by modeling the network as a graph, and computing all-pairs shortest paths on the edge weights of this graph. These distributed shortest-path routing algorithms describe the entire topology of the network, or a digest of it, to *all* routers on the network to find correct routes. On wired networks, such a requirement is intuitive, in the sense that wired links may be of arbitrary length, and may be placed in any arbitrary configuration among nodes, independently of the physical distance between nodes. Thus, one must search over the entire topological description of the network to be certain to find a path that exists. However, this communication of the network's topology to all nodes comes at the cost of routing protocol traffic. Moreover, routers need up-to-date topological information to find correct routes, so in the worst case, changes in

topology must be promptly described to all nodes in the network. On a properly functioning wired network, changes in the topology are infrequent; they are caused by node or link failures, or by decommissioning of old links or instatement of new ones. On wireless networks, however, the network topology varies frequently in the course of normal operation; mobility of nodes results in a constantly changing network topology, as nodes move into and out of one another's radio ranges.

A community of ad-hoc network researchers has proposed, implemented, and measured a variety of routing algorithms for such mobile, wireless networks. While these ad-hoc routing algorithms are designed to generate less routing protocol traffic than the above-mentioned shortest-path routing protocols in the face of a changing topology, they nevertheless compute shortest-path routes using either topological information concerning the entire network, or topological information concerning the entire set of currently used paths between sources and destinations. Thus, their ability to find routes depends similarly on describing the current wide-area topology of the network to routers.

We propose a different strategy for routing on wireless networks than these traditional routing algorithms and ad-hoc routing algorithms use. The central approach in this thesis is to make routing decisions using the *geographic positions* of nodes in the network, as first suggested by Nelson and Kleinrock [31], Hou and Li [15], and Finn [10]. By using geographic forwarding, we exploit the facts that:

- As the density of nodes on a wireless network increases, shortest paths between sources and destinations correspond increasingly closely to the Euclidean straight line between them.

- On wireless networks, the positions of *geographically nearby* nodes determine which links exist.

Intuitively, leveraging this inherent structure in wireless networks can localize the portion of the network topology that must be described to routers in a routing protocol. Localizing the topological information that must be communicated among routers in a routing protocol improves the scaling of routing in three ways: it reduces the absolute volume of routing protocol message traffic, reduces the size of the state that must be stored at routers, and reduces the risk that state stored at a router concerning a far-away portion of the topology will become stale. We propose Greedy Perimeter Stateless Routing (GPSR), a routing protocol for wireless networks, which makes geographic forwarding decisions, and finds routes using knowledge at each node of *only that node's immediate single-hop neighbors in the topology*.

1.1 Metrics for Evaluating Routing Scalability

Our aim is to show that GPSR is a highly *scalable* routing protocol. We aim for scalability under increasing numbers of nodes in the network, and increasing mobility rate. As these factors increase, our measures of scalability are:

- Routing protocol message cost: How many routing protocol packets does a routing algorithm send? This metric represents the overhead of routing—the reduction in network capacity for user data surrendered to maintenance of correct routes.
- Application packet delivery success rate: What fraction of applications' packets are

delivered successfully by a routing algorithm? This metric represents the useful work done by a routing algorithm.

- **Path length:** How long are the routes found by a routing algorithm, in comparison with the optimal shortest paths in the network graph? This metric represents how the latency experienced by applications' packets compares with the shortest possible. On wireless networks with fixed transmitter power (*e.g.*, today's commodity IEEE 802.11 (WaveLAN) radios), this metric also reveals the radio power consumed to deliver a packet from the source to the destination. In the case of GPSR, where we use topological information concerning only a node's immediate neighbors to make packet forwarding decisions, measuring path length reveals how much optimality is sacrificed to avoid routing protocol overhead.
- **Per-node state:** How much storage does a routing algorithm require at each node? This metric is somewhat untraditional in the routing protocol literature. However, on wireless networks comprised of resource-impooverished devices, such as low-power sensors, keeping small state at each node is essential, even when the number of deployed sensors in a network is vast.

1.2 Traditional Shortest-Path Algorithms

The two main categories of shortest-path routing algorithms, Distance-Vector (DV, also known as Distributed Bellman-Ford, DBF) [14] and Link-State (LS) [28] algorithms, require continual distribution of a current map of the entire network's topology to all routers.

DV's Bellman-Ford approach constructs this global picture transitively; each router includes its distance (the sum of the edge weights between it and the destination) from all network destinations in each of its periodic beacons. Receipt of a beacon containing a routing table entry for a destination implies that the receiver can route to that destination via the neighbor from whom that beacon was received, at a cost equal to the sum of the distance in the routing table entry and cost of the link over which the beacon was received. Over time, the route for a destination propagates outward by one hop each time a router sends its next beacon after learning a route for that new destination. After enough beaconing rounds, all nodes learn routes for all destinations they can reach.

LS's Dijkstra approach directly floods announcements of the change in any link's status to every router in the network. Each router keeps a map of the entire network graph, and runs Dijkstra's algorithm on this graph map.

Small inaccuracies in the state at a router under both DV and LS can cause routing loops or disconnection [42]. When the topology is in constant flux, as under mobility, LS generates torrents of link status change messages, and DV either suffers from out-of-date state [7], or generates torrents of triggered updates— messages sent upon change of a metric for a destination, before the full inter-beacon interval has passed.

1.3 Ad-Hoc Routing Algorithms

A wide variety of ad-hoc routing algorithms have been proposed in the literature. By way of introduction, we focus on Dynamic Source Routing (DSR) [18]; we compare GPSR with DSR later in the thesis, because DSR has been shown to perform better than many

other published routing algorithms [7]. In DSR, packets are routed using *source routes*; each packet contains the full sequence of hops it is to take from the source node to the destination node. Forwarding such a packet amounts to finding the next hop in the list of hops, and sending the packet to the appropriate neighbor. The task of writing the full route into the packet falls to the packet's originator. If a node originates a packet, and does not already know a route to the destination, it floods a *route request* packet to all nodes in the network. As a route request propagates, it records all hops it traverses. When a route request reaches the destination, the destination node replies to the request's originator with the reversed list of hops accumulated by the request. This reversed list is the source route from the source to the destination. Note that DSR only generates routing protocol traffic in response to demand for forwarding to an unknown destination. Thus, DSR is an *on-demand* routing protocol, whereas traditional DV and LS algorithms are *pro-active*, and continually describe the topology to all nodes the network.

When a source route to a destination breaks, because two adjacent nodes in the source route cease to be neighbors, the node who no longer has the next-hop neighbor sends a *route error* to the packet's originator. In response, the packet's originator re-queries to learn up-to-date source routes for the destination.

To reduce the traffic load of route queries, all nodes aggressively *cache* all routes they overhear. When a route request arrives for a destination in the route cache, a route reply is sent to the requestor without propagating the route request further. We discuss the implications of this caching behavior in the next section.

1.4 Techniques for Routing Scalability

The two dominant factors in the scaling of both traditional shortest-path routing algorithms and ad-hoc routing algorithms like DSR are:

- The rate of change of the topology.
- The number of routers in the routing domain.

Both factors affect the message complexity of DV and LS routing algorithms: intuitively, pushing current state globally costs packets proportional to the product of the rate of state change and number of destinations for the updated state. In the case of DSR, source routes break more frequently as mobility increases, and the probability that a source route breaks increases as the network diameter increases.

Two main approaches are used in an attempt to mitigate the influence of these two factors in limiting the scalability of routing protocols:

- *Hierarchy* is the most widely deployed approach to scale routing as the number of network destinations increases. Without hierarchy, Internet routing could not scale to support today's number of Internet leaf networks. An Autonomous System runs an intra-domain routing protocol inside its borders, and appears as a single entity in the backbone inter-domain routing protocol, BGP. This hierarchy is built on well-defined and rarely changing administrative and topological boundaries. *The assumptions that such static boundaries exist, and that a common administrative authority can set them, are incorrect on freely moving ad-hoc wireless networks.*

- *Caching* has come to prominence as a strategy for scaling ad-hoc routing protocols. Dynamic Source Routing (DSR) [18], Ad-Hoc On-Demand Distance Vector Routing (AODV) [33], and the Zone Routing Protocol (ZRP) [13] all eschew constantly pushing current topology information network-wide. Instead, routers running these protocols request topological information in an *on-demand* fashion as required by their packet forwarding load, and cache it aggressively. When their cached topological information becomes out-of-date, these routers must obtain more current topological information to continue routing successfully. Caching reduces the routing protocols' message load in two ways: it avoids pushing topological information where the forwarding load does not require it (*e.g.*, at idle routers), and it often reduces the number of hops between the router that has the needed topological information and the router that requires it (*i.e.*, a node closer than a changed link may already have cached the new status of that link). *Caching in computer systems is predicated on the assumption that cached values remain valid long enough to be reused before becoming stale. This assumption becomes invalid as mobility and the length of a route increase in the limit; the probability that a cached route remains correct is inversely proportional to the product of the mobility rate and path length.*

1.5 Applicability of Scalable Wireless Routing

Wireless networks that push on mobility, number of nodes, or both include:

- Ad-hoc networks: Perhaps the most investigated category, these mobile networks have no fixed infrastructure, and support applications for military users, post-disaster

rescuers, and temporary collaborations among temporary associates, as at a business conference or lecture [13], [18], [32], [33], [34].

- **Sensor networks:** Comprised of small sensors, these mobile networks can be deployed with very large numbers of nodes, and have very impoverished per-node resources [9], [19]. Minimization of state per node in a network of tens of thousands of memory-poor sensors is crucial.
- **“Rooftop” networks:** Proposed by Shepard [37], these wireless networks are not mobile, but are deployed very densely in metropolitan areas (the name refers to an antenna on each building’s roof, for line-of-sight with neighbors) as an alternative to wired networking offered by traditional telecommunications providers. Such a network also provides an alternate infrastructure in the event of failure of the conventional one, as after a disaster. A routing system that self-configures (without a trusted authority to configure a routing hierarchy) for hundreds of thousands of such nodes in a metropolitan area represents a significant scaling challenge.
- **Vehicular networks:** These networks consist of moving vehicles equipped with radios [29]. Both peer-to-peer communication, as for music sharing and driver-to-driver communication, and Internet access infrastructure uses, in which vehicles reach base stations connected to the Internet via routes through other vehicles, are useful applications on such networks. The availability of the vehicle battery as a power source, recharged by generation of current from the vehicle’s propulsion system, eliminates the need for concern about battery life limitations at nodes.

1.6 Assumptions

We assume in this work that all wireless routers know their own positions, either from a GPS device, if outdoors, or through other means. Practical solutions include surveying, for stationary wireless routers; inertial sensors, on vehicles, as are commonly deployed in car mapping and navigation systems; and acoustic range-finding using ultrasonic “chirps” indoors [41], [35]. We further assume bidirectional radio reachability. The widely used IEEE 802.11 wireless network MAC [17] sends link-level acknowledgements for all unicast packets, so that all links in an 802.11 network must be bidirectional. We simulate a network that uses 802.11 radios to evaluate our routing protocol. We consider topologies where the wireless nodes are roughly in a plane. We assume that the distance between nodes determines whether a link exists between them; below a certain distance threshold, two nodes are within range of one another. Finally, we assume that packet sources can determine the approximate locations (to within a radio range) of packet destinations, to mark packets they originate with their destination’s location. Thus, we assume a location registration and lookup service that maps node addresses to locations [25]. Queries to this system use the *same* geographic routing system as data packets; the querier geographically addresses his request to a location server. The scope of this thesis is limited to geographic routing. We discuss interaction with the location service briefly in Section 5.2. A technique for correcting for inaccuracy in the position of the destination is presented in Section 5.3. We adopt IP terminology throughout, though GPSR can be applied to any datagram network.

1.7 Thesis Contents

We will show that geographic routing allows routers to be nearly stateless, and requires propagation of topology information for only a *single hop*: each node need only know its neighbors' positions. The self-describing nature of position is the key to geography's usefulness in routing. The position of a packet's destination and positions of the candidate next hops are sufficient to make correct forwarding decisions, without any other topological information. This self-describing property of geographic addresses is in contrast with usual flat network addresses (as in the "default-free" core of the Internet), the internal structure of which does not assist in making forwarding decisions, such that routers must make table lookups to choose a next hop.

In Chapter 2, we describe a simple greedy geographic forwarding algorithm, discuss the scalability implications of its design, and evaluate the algorithm's degree of success in finding routes on static, non-mobile wireless networks. This greedy algorithm does not always find paths successfully; we characterize the topologies on which this is the case.

In Chapter 3, motivated by the failures of greedy forwarding, we propose two methods for recovering from greedy forwarding failure. The first method, perimeter probing, uses a heuristic to remove crossing links from the wireless network, and finds most routes successfully, but not all. We characterize the topologies where perimeter probing fails to find routes. The second method, planarization of the graph, finds all routes successfully on static networks. We then present the full GPSR algorithm, which combines greedy forwarding where topology allows, with forwarding along perimeters of the planarized graph, where greedy forwarding is impossible.

In Chapter 4, we evaluate GPSR in simulation on dense mobile wireless networks of 50, 112, and 200 nodes, at varying degrees of motion, including simulation of the full IEEE 802.11 physical and MAC layers, using the scalability metrics proposed in this introduction. We also simulate a sparser configuration of nodes. We show that GPSR keeps tiny state per node, delivers user packets robustly, generates small routing protocol overhead, and delivers the vast majority of packets in the number of hops equal to that along the shortest path. We simulate DSR for comparison on the same networks, and show that GPSR outperforms DSR by these metrics.

In Chapter 5, we discuss the properties of GPSR, and describe avenues for further extension of the work in this thesis.

We review related work in Chapter 6.

Finally, we conclude in Chapter 7, by reviewing the design of GPSR, summarizing the results of our evaluation of GPSR, and stating the contributions of this thesis.

Chapter 2

Greedy Forwarding

We now describe the first part of the Greedy Perimeter Stateless Routing algorithm: *greedy forwarding*. In this chapter, we define the greedy forwarding rule; define a simple beaconing protocol for nodes to learn their neighbors' positions; identify the desirable properties of greedy forwarding; define the topologies on which greedy forwarding fails; and characterize the frequency of greedy forwarding failure by the *density* of nodes in a network.

2.1 Greedy Forwarding Rule

As alluded to in the introduction, under GPSR, packets are marked by their originator with their destinations' locations. As a result, a forwarding node can make a locally optimal, greedy choice in choosing a packet's next hop. Specifically, if a node knows its radio neighbors' positions, the locally optimal choice of next hop is the neighbor geographically closest to the packet's destination. Forwarding in this regime follows successively closer geographic hops, until the destination is reached. An example of greedy next-hop choice

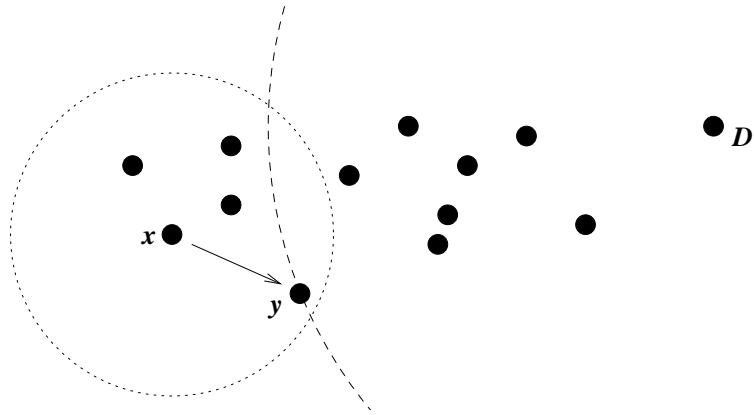


Figure 2.1: Greedy forwarding example. y is x 's closest neighbor to D .

appears in Figure 2.1. Here, x receives a packet destined for D . x 's radio range is denoted by the dotted circle about x , and the arc with radius equal to the distance between y and D is shown as the dashed arc about D . x forwards the packet to y , as the distance between y and D is less than that between D and any of x 's other neighbors. This greedy forwarding process repeats until the packet reaches D .

Suppose the header of a packet p contains fields $p.a$, the address of the packet's destination, and $p.l$, the location of the packet's destination. Moreover, assume for the moment that each node has a neighbor table N , each of whose entries is a pair of a neighbor node's address (a) with that neighbor's location (l). We denote a node's own address and location by $\text{self}.a$ and $\text{self}.l$. A formal statement of the greedy forwarding rule is shown in Figure 2.2.

2.2 Beaconing Protocol

A simple beaconing protocol provides all nodes with their neighbors' positions: periodically, each node transmits a beacon to the broadcast MAC address, containing only its own

```

GREEDY-FORWARD( $p$ )
1   $n_{\text{best}} = \text{self}.a$ 
2   $d_{\text{best}} = \text{DISTANCE}(\text{self}.l, p.l)$ 
3  for each ( $a, l$ ) in  $N$ 
4  do  $d = \text{DISTANCE}(l, p.l)$ 
5     if  $a == p.a$  or  $d < d_{\text{best}}$ 
6     then  $n_{\text{best}} = a$ 
7          $d_{\text{best}} = d$ 
8     if  $a == p.a$ 
9     then break
10 if  $n_{\text{best}} == \text{self}.a$ 
11 then return greedy forwarding failure
12 else forward  $p$  to  $n_{\text{best}}$ 
13 return greedy forwarding success

```

Figure 2.2: Greedy forwarding rule pseudocode. $\text{DISTANCE}(e, f)$ computes the Euclidean distance between nodes e and f —in two dimensions, $\sqrt{(x_e - x_f)^2 + (y_e - y_f)^2}$.

identifier (e.g., IP address) and position. We encode position as two four-byte floating-point quantities, for x and y coordinate values. To avoid synchronization of neighbors’ beacons, as observed by Floyd and Jacobson [11], we jitter each beacon’s transmission by 50% of the interval B between beacons, such that the mean inter-beacon transmission interval is B , uniformly distributed in $[0.5B, 1.5B]$.

Upon not receiving a beacon from a neighbor for longer than timeout interval T , a GPSR router assumes that the neighbor has failed or gone out-of-range, and deletes the neighbor from its table. The 802.11 MAC layer also gives direct indications of link-level retransmission failures to neighbors; we interpret these indications identically. We have used $T = 4.5B$, three times the maximum jittered beacon interval, in this work.

The position a node associates with a neighbor becomes less current between beacons as that neighbor moves. The accuracy of the set of neighbors also decreases; old neighbors may leave and new neighbors may enter radio range. For these reasons, the correct choice

of beaconing interval to keep nodes' neighbor tables current depends on the rate of mobility in the network and range of nodes' radios. We show the effect of this interval on GPSR's performance in our simulation results. We note that keeping current topological state for a one-hop radius about a router is the minimum required to do *any* routing; no useful forwarding decision can be made without knowledge of the topology one or more hops away.

This beaconing mechanism does represent pro-active routing protocol traffic, avoided by DSR and AODV. To minimize the cost of beaconing, GPSR piggybacks the local sending node's position on *all* data packets it forwards, and runs all nodes' network interfaces in promiscuous mode, so that each station receives a copy of all packets for all stations within radio range. At a small cost in bytes (twelve bytes per packet), this scheme allows all packets to serve as beacons. When any node sends a data packet, it can then reset its inter-beacon timer. This optimization reduces beacon traffic in regions of the network actively forwarding data packets. Running network interfaces in promiscuous mode consumes power; we do not measure power consumption in this work.

In fact, we could make GPSR's beacon mechanism fully reactive by having nodes solicit beacons with a broadcast "neighbor request" only when they have data traffic to forward. We have not felt it necessary to take this step, however, as the one-hop beacon overhead does not congest our simulated networks.

2.3 Advantages of Greedy Forwarding

Greedy forwarding's great advantage is its reliance only on knowledge of the forwarding node's immediate neighbors. The state required is negligible, and dependent on the density of nodes in the wireless network, not the total number of destinations in the network.¹ On networks where multi-hop routing is useful, the number of neighbors within a node's radio range must be substantially less than the total number of nodes in the network.

As mentioned in the Introduction, as the density in space of the nodes deployed on a wireless network increases, greedy forwarding approximates shortest paths progressively more closely; the shortest path between two nodes tends toward the Euclidean straight line between them, as the minimum possible number of hops is bounded below by the number of radio ranges between source and destination, laid end-to-end.

Traditional shortest-path routing algorithms cannot exploit structure in IP addresses to make forwarding decisions; they must treat IP addresses as flat identifiers, and resort to a table lookup among all destinations in the routing domain. It is the self-describing nature of geographic coordinates that allows forwarding routers to interpret the destination location in a packet to make a purely local forwarding decision.

Note that the only routing protocol traffic required for greedy forwarding is that of the beaconing protocol. Because the beaconing protocol pushes state only a single hop in the network, intuitively it should consume considerably less bandwidth than protocols which distribute state globally throughout the routing domain (*e.g.*, DV and LS routing protocols), or accumulate state along an entire source route (*e.g.*, DSR).

¹The word "stateless" in GPSR's name is not meant literally, but refers to this small, purely local state.

Because greedy forwarding makes purely local decisions, it should be robust under topological changes; a node can make correct forwarding decisions without requiring up-to-date state (or indeed, any state) concerning nodes beyond a single hop away.

2.4 Limits to Greedy Forwarding’s Applicability: Voids

The power of greedy forwarding to route using only neighbor nodes’ positions comes with one attendant drawback: there are topologies in which the only route to a destination requires a packet move temporarily *farther* in geometric distance from the destination [10], [22]. A simple example of such a topology is shown in Figure 2.3. Here, x is closer to D than its neighbors w and y . Again, the dashed arc about D has a radius equal to the distance between x and D . Although two paths, $(x \rightarrow y \rightarrow z \rightarrow D)$ and $(x \rightarrow w \rightarrow v \rightarrow D)$, exist to D , x will not choose to forward to w or y using greedy forwarding. x is a local maximum in its proximity to D . Some other mechanism must be used to forward packets in these situations.

Motivated by Figure 2.3, we note that the *intersection* of x ’s circular radio range and the circle about D of radius $|\overline{xD}|$ (that is, of the length of line segment \overline{xD}) is empty of neighbors. We show this region clearly in Figure 2.4. From node x ’s perspective, we term the shaded region without nodes a *void*. x seeks to forward a packet to destination D beyond the edge of this void. Intuitively, x seeks to route *around* the void; if a path to D exists from x , it doesn’t include nodes located within the void (or x would have forwarded to them greedily).

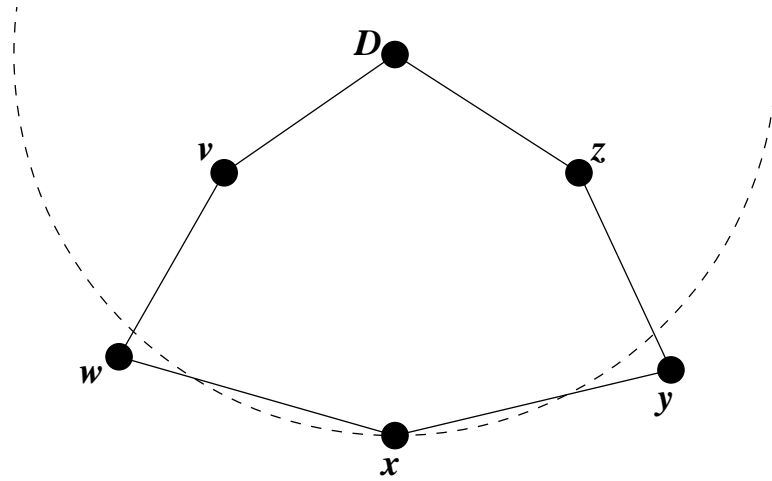


Figure 2.3: Greedy forwarding failure. x is a local maximum in its geographic proximity to D ; w and y are farther from D .

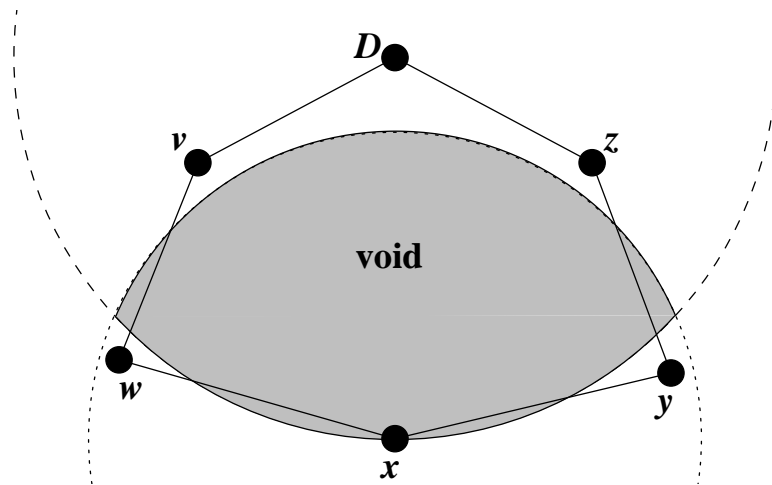


Figure 2.4: Node x 's *void* with respect to destination D .

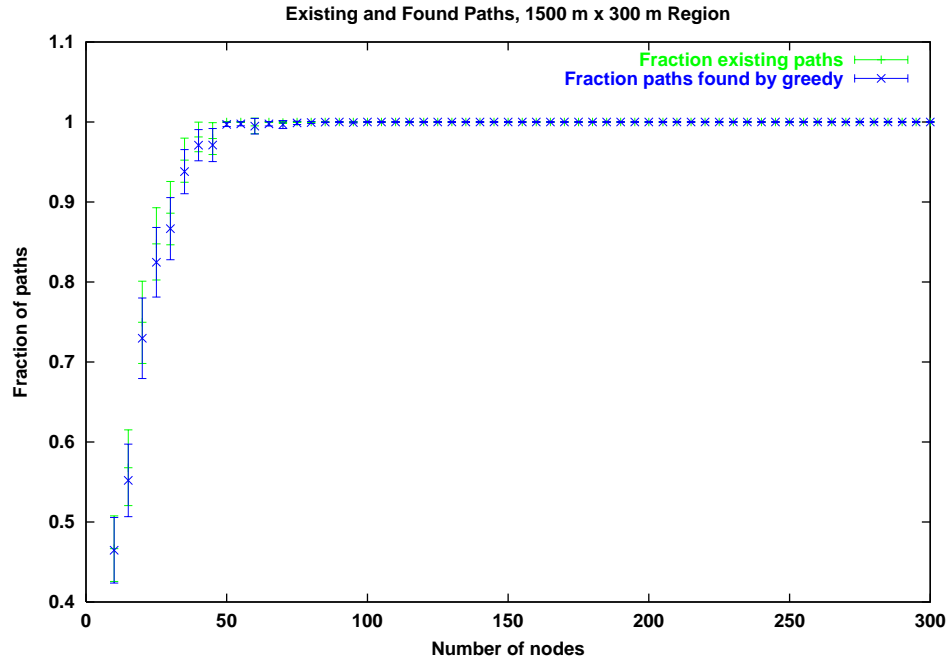


Figure 2.5: Existing paths and greedy paths, 1500 m by 300 m region. 10–300 nodes, in increments of 5. Radio range is 250 m.

2.5 Simulations: The Role of Density

In Figures 2.5, 2.6, 2.7, and 2.8, we present idealized simulations of static (non-mobile) networks to illustrate the relationship between the density of the nodes deployed in a wireless network and the frequency with which greedy forwarding succeeds. The simulations are idealized in the sense that they do not model the physical channel’s or MAC layer’s capacity or contention behavior. Rather, the intent behind these simulations is to show the inherent limitations of greedy forwarding in finding routes in the presence of voids, even over a perfect (infinite capacity) wireless network.

In these simulations, varying numbers of nodes are placed uniformly at random in a region. We investigate four region sizes: 1500 m by 300 m; 670 m by 670 m; 3000 m by 600 m; and 1340 m by 1340 m. These region sizes represent 1:1 and 5:1 aspect ratios, in two

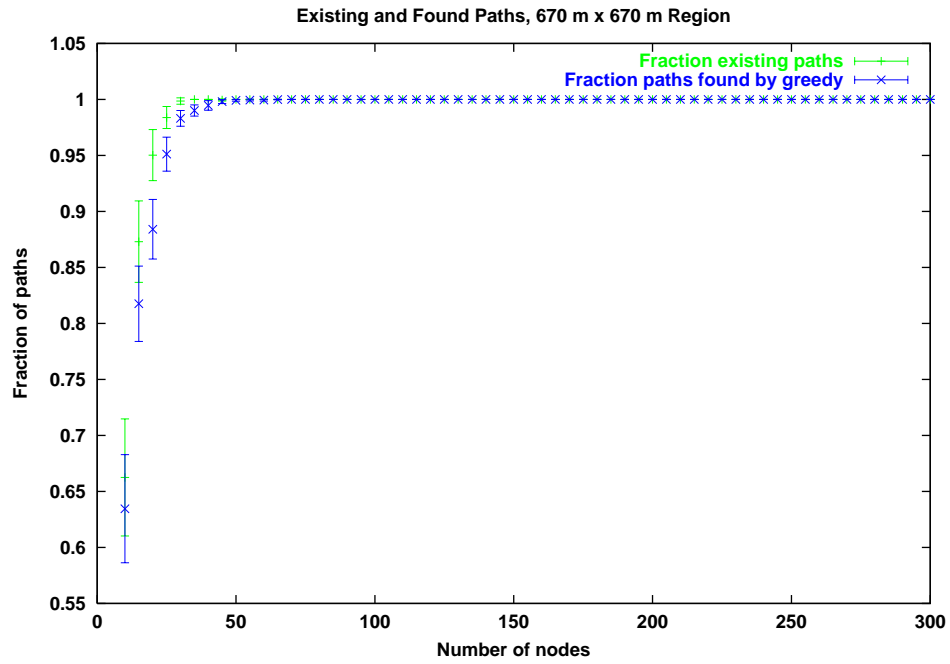


Figure 2.6: Existing paths and greedy paths, 670 m by 670 m region. 10–300 nodes, in increments of 5. Radio range is 250 m.

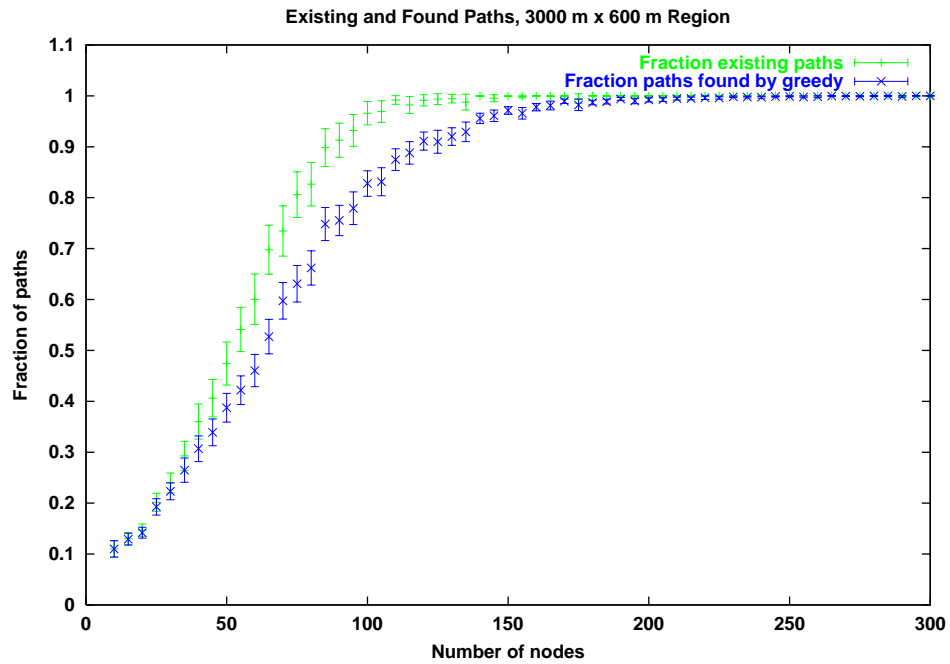


Figure 2.7: Existing paths and greedy paths, 3000 m by 600 m region. 10–300 nodes, in increments of 5. Radio range is 250 m.

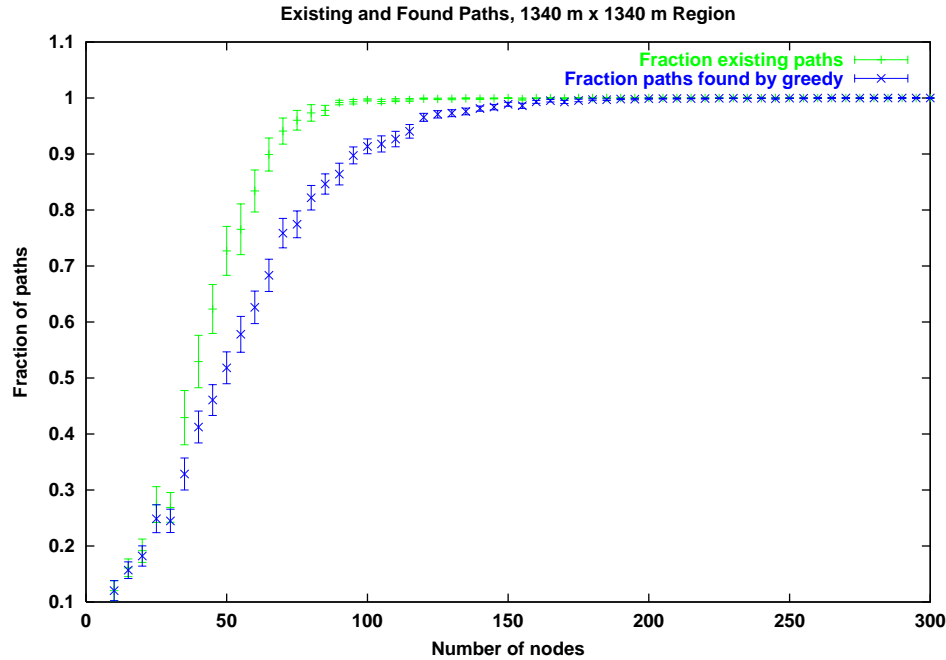


Figure 2.8: Existing paths and greedy paths. 1340 m by 1340 m region. 10–300 nodes, in increments of 5. Radio range is 250 m.

total areas. The 5:1 regions have the same aspect ratio as the regions used in simulations of DSR, against which we compare GPSR later in this thesis. Radio range is fixed at 250 m, the characteristic range of IEEE 802.11 DSSS radios.

Using the 250 m distance as a threshold for the presence or absence of a link between all pairs of nodes, we induce a connectivity graph in each simulation. We use Floyd-Warshall to compute how many of the possible $n(n - 1)$ paths exist. We then attempt to use greedy forwarding as described above to find all of these existing paths. In each graph, we present the fraction of the $n(n - 1)$ possible paths that exist in the topology, as found by Floyd-Warshall, and the fraction of the $n(n - 1)$ possible paths found by greedy forwarding. Each point represents the mean of 90 simulations on different randomly generated topologies, and includes the 97.5% confidence interval for this mean as an error bar.

All four region sizes demonstrate the same trend: greedy forwarding tends to find all routes on the sparsest networks and the densest networks, but fails to find some routes in a middle range of node densities. On very sparse networks, there are so few nodes, and hence routes on average consist of so few hops, that voids are very rarely on a path between a source and a destination. Note from the previous section that voids occur when two overlapping circles are empty of nodes. The probability that this overlapping region is empty decreases as nodes become thicker on the ground. Hence, greedy forwarding tends toward finding all routes as the density of nodes increases.

The aspect ratio of the region has an effect on the success rate of greedy forwarding in finding routes. In the 1500-m-by-300-m simulations (Figure 2.5), the vertical dimension of the simulated region is not much longer than the 250 m radio range. Very few voids can exist in such a region, where one node's radio range covers nearly the entire y dimension of the region. Hence, greedy forwarding finds a greater proportion of the existing routes in this region than in the others measured.

Chapter 3

The Right-Hand Rule: Perimeters

In this chapter, we address the failure of pure greedy routing to find paths in the presence of voids, by introducing two *perimeter traversal* algorithms for forwarding packets *around* voids. After describing the *right-hand rule* for traversing a graph, we characterize the behavior of the right-hand rule on wireless network graphs, and observe the role played by crossing edges in the graph in interfering with the right-hand-rule traversal. We then introduce *perimeter probing*, an algorithm that probes and maps the positions of nodes that border voids, while employing a *no-crossing heuristic* to eliminate crossing edges from the graph, and uses the resulting state to forward around voids. Drawing on existing results from computational geometry, we describe the *Gabriel Graph* and *Relative Neighborhood Graph* planar graphs, and introduce distributed algorithms for identifying these graphs as subsets of a wireless network graph. Finally, after describing the topologies on which perimeter probing fails to find routes, we introduce a superior algorithm, *planar face traversal*, that finds *all* routes on a static network by forwarding only on planar subsets of

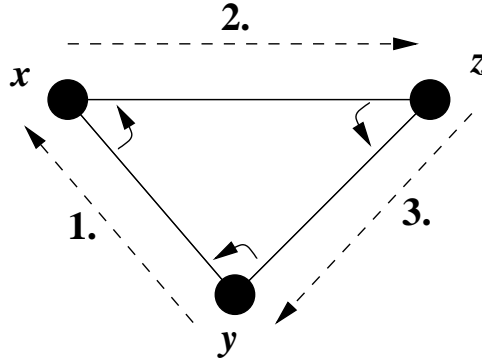


Figure 3.1: The right-hand rule (*interior* of the triangle). x receives a packet from y , and forwards it to its first neighbor counterclockwise about itself, z , &c.

the wireless network graph's edges. Planar face traversal allows recovery from all cases of greedy failure, while only requiring state concerning the positions of a node's immediate neighbors.

3.1 The Right-Hand Rule

The long-known *right-hand rule* for traversing a graph is depicted in Figure 3.1. This rule states that when arriving at node x from node y , the next edge traversed is the next one sequentially counterclockwise about x from edge (x,y) . It is known that the right-hand rule traverses the interior of a closed polygonal region (a *face*) in clockwise edge order—in this case, the triangle bounded by the edges between nodes x , y , and z , in the order $(y \rightarrow x \rightarrow z \rightarrow y)$. The rule traverses an exterior region, in this case, the region *outside* the same triangle, in counterclockwise edge order.

For a network node with a list of its neighbors' positions, forwarding a packet that arrives from a neighbor at bearing b_{in} by the right-hand rule amounts to choosing the neighbor whose bearing b_{out} minimizes the difference $b_{\text{in}} - b_{\text{out}}$, where bearings are defined

```

RIGHT-HAND-FORWARD( $p, n_{\text{in}}$ )
1   $b_{\text{in}} = \text{NORM}(\text{ATAN2}(\text{self}.l.y - n_{\text{in}}.y, \text{self}.l.x - n_{\text{in}}.x))$ 
2   $\delta_{\text{min}} = 3\pi$ 
3  for each ( $a, l$ ) in  $N$ 
4  do if  $a == n_{\text{in}}$ 
5      then continue
6       $b_a = \text{NORM}(\text{ATAN2}(\text{self}.l.y - l.y, \text{self}.l.x - l.x))$ 
7       $\delta_b = \text{NORM}(b_a - b_{\text{in}})$ 
8      if  $\delta_b < \delta_{\text{min}}$ 
9          then  $\delta_{\text{min}} = \delta_b$ 
10              $a_{\text{min}} = a$ 
11 return  $a_{\text{min}}$ 

```

Figure 3.2: Right-hand rule forwarding pseudocode. `NORM` normalizes its argument in radians into $[0, 2\pi]$ by repeatedly adding 2π . `ATAN2(y, x)` computes the arc tangent of y/x in the appropriate quadrant (after the UNIX C math library function).

on $[0, 2\pi]$. Pseudocode for forwarding a packet p that has arrived from neighbor n_{in} by the right-hand rule appears in Figure 3.2. When two neighbors are located along the exact same bearing, the geographically closer neighbor is used as the next hop.

We seek to exploit these cycle-traversing properties to route around voids. In Figure 2.4, traversing the cycle ($x \rightarrow w \rightarrow v \rightarrow D \rightarrow z \rightarrow y \rightarrow x$) by the right-hand rule amounts to navigating *around the pictured void*, specifically, to nodes closer to the destination than x (in this case, including the destination itself, D). We call the sequence of edges traversed by the right-hand rule a *perimeter*.

Unfortunately, the right-hand rule does not yield a traversal of the perimeter of a closed polygon on all wireless network graphs. On graphs with edges that cross, the right-hand rule may instead take a degenerate tour of edges that does not trace the boundary of a closed polygon. Such graphs with crossing edges are known as *non-planar* graphs, or

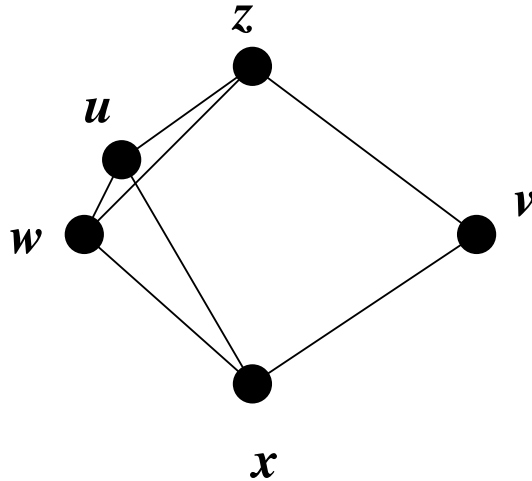


Figure 3.3: A network with crossing edges. Starting from x to u , the right-hand rule gives the tour: $(x \rightarrow u \rightarrow z \rightarrow w \rightarrow u \rightarrow x)$.

more precisely, non-planar embeddings of graphs¹; for brevity, we refer to them as non-planar graphs herein. An example of a non-planar graph appears in Figure 3.3. Here, when x originates a packet to u , the right-hand rule results in the tour: $(x \rightarrow u \rightarrow z \rightarrow w \rightarrow u \rightarrow x)$. The problem is the crossing edges: (w, z) and (u, x) . If (w, z) were removed from the graph, the perimeter probe from x to u would instead have taken the desired tour, $(x \rightarrow u \rightarrow z \rightarrow v \rightarrow x)$.

We introduce the *no-crossing heuristic*: if, during traversal of a graph by the right-hand rule, the candidate next edge crosses an edge taken earlier in the traversal, that candidate next edge is ignored, and the *next* edge in counterclockwise order is taken, instead. The purpose of this heuristic is to remove crossing edges from the graph, so that the right-hand rule takes the intended tour. In the case of Figure 3.3, starting from x , after taking the path $(x \rightarrow u \rightarrow z)$, the no-crossing heuristic ignores edge (z, w) at z , because it crosses

¹A planar embedding of a graph is a placement of its vertices in a plane, made while preserving the graph's edges. A planar graph has at least one planar embedding in which no edges cross. A non-planar graph has no planar embedding in which no edges cross.

the previously taken edge (x, u) . Here, the heuristic has the desired effect: the complete clockwise outer edge tour $(x \rightarrow u \rightarrow z \rightarrow v \rightarrow x)$ is taken. The implementation of this heuristic is straightforward: each node appends its location to packets it forwards by the right-hand rule, and checks whether a candidate next edge crosses one already taken in the packet's path history using simple simultaneous equations for the two edges in question. We omit these details in Figure 3.2.

3.2 Perimeter Probing

Building on the right-hand rule and no-crossing heuristic, we now describe *perimeter probing*, through which nodes pro-actively map the perimeters they border, and use this knowledge of the local topology to attempt to recover from greedy forwarding failure by routing around voids.

3.2.1 Greedy Perimeter Probing (GPP) Algorithm

In the topology in Figure 2.4, suppose x sends a *perimeter probe* packet to w . At each hop, the packet is forwarded using the right-hand rule with the no-crossing heuristic, and each forwarding router appends its address and position to the packet. When the packet returns to x , it will contain a list of the positions and addresses of all nodes on the perimeter. Node x consumes the packet and caches this state. A proof that perimeter probe packets forwarded in this fashion on static network topologies *always* return to their originator can be found in [30].

Thereafter, should a packet arrive at x for greedy forwarding to D , x can “fail-over” to

use the perimeter it has learned, which includes nodes v , D , and z , all of which are closer to D than x . Node x can either source-route the packet to any node closer to D on the cached perimeter, or mark the packet for forwarding by the right-hand rule, so that it takes the same path as the earlier perimeter probe packet. In this way, the packet will reach a node closer to D than x , where greedy forwarding can resume.

More generally, we can augment greedy forwarding with perimeter probing, in an effort to recover from greedy forwarding failure by forwarding along perimeters. All nodes periodically originate a perimeter probe packet (marked *perimeter probe* in a packet p 's packet mode field, $p.M$, as in Table 3.1) to each of their neighbors, and cache the perimeters stored in these packets when they return to their originators. Greedy forwarding is used for all data packets where possible—that is, by all nodes where there exists a neighbor closer to the destination. When no such neighbor exists, a node searches its cached list of perimeters for any node closer than itself to the destination. If there is no closer node on any perimeter, no route is known, and the node drops the packet. If such a closer node n_c exists along perimeter p_c , the packet's mode field $p.M$ is changed to *perimeter data*, and the packet is marked in $p.i$ with the location where this mode transition occurred. It is then forwarded to the next node along p_c . Each successive node that receives a perimeter-mode packet forwards the packet by the right-hand rule, until the packet reaches a node closer to the destination $p.D$ than that where it entered perimeter mode (at $p.i$). At that closer node, the packet is returned to *greedy mode*, and greedy forwarding continues thereafter. Thus, the sequence of hops a packet takes in perimeter mode in the aggregate acts as a single greedy hop, as the packet reaches a node closer to the destination than the one where it en-

Field	Function
s	Source Address
d	Destination Address
D	Destination Location (x, y)
M	Packet Mode (perimeter probe; greedy data; perimeter data)
i	Location Packet Entered Perimeter Mode

Table 3.1: Fields in GPP packets.

tered perimeter mode, in accordance with the greedy forwarding criterion. Pseudocode for mixed greedy/perimeter forwarding, which we name the GPP (Greedy Perimeter Probing) algorithm, appears in Figure 3.4. The packet fields used by GPP are shown in Table 3.1. Note that all data packets begin in greedy mode, with their M field set to *greedy data*.

A simple example of the operation of GPP, based on Figure 2.4, is shown in Figure 3.5. Node S originates a data packet to D . The first hop (S, x) is greedy. Because x is a local maximum, x must use the perimeter it learned from an earlier perimeter probe. Node x marks the packet in perimeter mode, records its own position in the packet, and passes the packet to w , the first hop on the perimeter. Node w is not closer to D than x , so w right-hand-rule forwards the perimeter mode packet to v . As v is closer to D than x , v marks the packet in greedy mode, and forwards it greedily to D .

3.2.2 Simulation and Evaluation of GPP

To evaluate the performance of GPP, we simulate the algorithm in an idealized (contentionless, infinite-bandwidth) simulator on static (non-mobile) networks. We also simulate a simple Distance-Vector (DV) routing algorithm. As was the case in the idealized simulations of greedy forwarding in the preceding chapter, this simulator places varying numbers

```

PERI-CLOSER-LOOKUP( $l$ )
1   $i_{\text{best}} = \text{NIL}$ 
2   $d_{\text{best}} = \text{DISTANCE}(\text{self}.l, l)$ 
3  for each  $i \in P$ 
4  do for each  $j \in i$ 
5      do  $d = \text{DISTANCE}(j, l)$ 
6          if  $d < d_{\text{best}}$ 
7              then  $i_{\text{best}} = i$ 
8                   $d_{\text{best}} = d$ 
9  return  $i_{\text{best}}$ 

GPP-FORWARD( $p, n_{\text{in}}$ )
1  if  $p.d == \text{self}.a$ 
2      then receive packet
3  else switch
4      case  $p.M == \text{greedy data} :$ 
5          if  $\text{GREEDY-FORWARD}(p) == \text{failure}$ 
6              then if  $(p_c = \text{PERI-CLOSER-LOOKUP}(p.D)) \neq \text{NIL}$ 
7                  then  $p.M = \text{perimeter data}$ 
8                       $p.i = \text{self}.l$ 
9                      forward  $p$  along  $p_c$ 
10                 else drop packet; destination unreachable
11     case  $p.M == \text{perimeter data} :$ 
12         if  $\text{DISTANCE}(\text{self}.l, p.D) < \text{DISTANCE}(p.i, p.D)$ 
13             then  $p.M = \text{greedy data}$ 
14                  $\text{GREEDY-FORWARD}(p)$ 
15             else  $t = \text{RIGHT-HAND-FORWARD}(p, n_{\text{in}})$ 
16                 forward  $p$  to  $t$ 
17     case  $p.M == \text{perimeter probe} :$ 
18         if  $p.s == \text{self}.a$ 
19             then consume  $p$ ; cache perimeter
20         else  $t = \text{RIGHT-HAND-FORWARD}(p, n_{\text{in}})$ 
21             forward  $p$  to  $t$ 

```

Figure 3.4: The GPP (Greedy Perimeter Probing) algorithm: PERI-CLOSER-LOOKUP and GPP-FORWARD.

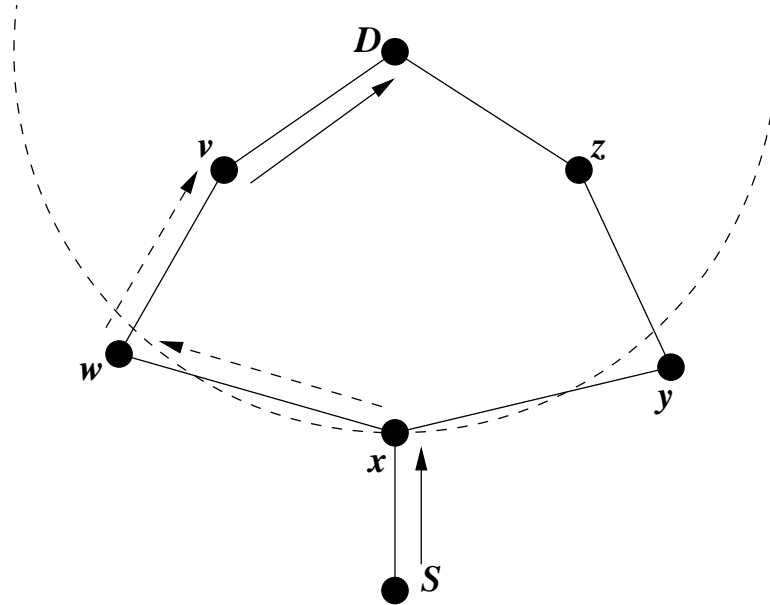


Figure 3.5: Mixed forwarding. Solid arrows are greedy-mode hops; dashed arrows are perimeter-mode hops.

of nodes at random in a region of fixed size, and uses a threshold distance between nodes to induce a connectivity graph. Here, again, varying the number of nodes varies the node density. In these simulations, the threshold distance for radio connectivity is 250 m, and the size of the region on which nodes are placed randomly is 2500 m by 2500 m.

Because there is no packet loss and unlimited capacity on the simulated network, and because both routing algorithms are allowed to converge fully before measurements are taken, these measurements represent the ideal behavior of GPP and DV: none of the challenges of finding routes when routing protocol packets may be lost, or when changes in the topology cause changes in routes, occur here. GPP's perimeter probing with the no-crossing heuristic is meant to recover from greedy forwarding failure, while accumulating less state per node than in traditional routing algorithms, such as DV and LS routing, which hold state proportional to the number of network destinations in each router. To examine

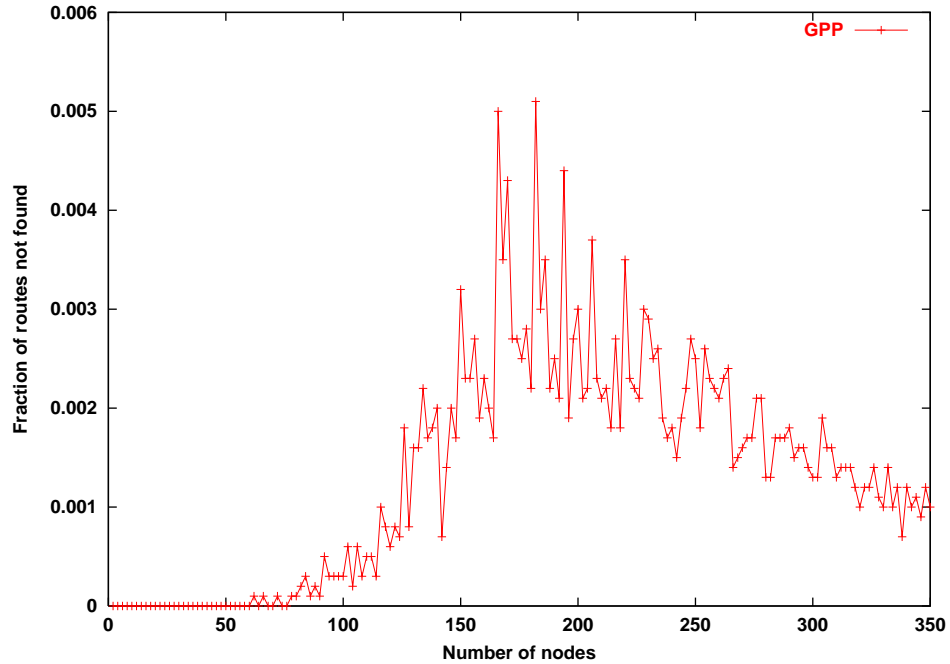


Figure 3.6: Percentage of all n^2 routes *not* found, GPP.

GPP’s performance in these two areas, in these simulations we measure the percentage of routes found by the GPP algorithm and the size of the state (neighbor lists and perimeters) accumulated by the GPP algorithm at each node. Figures 3.6 and 3.7 show these measurements, respectively.

Note that GPP does not find all routes that exist, even on static network topologies. We describe the topologies where GPP fails in the next section. On the least dense networks, GPP finds all routes. However, as density first increases, GPP finds progressively fewer routes, eventually peaking at approximately 0.5% of all n^2 routes not found at 180 nodes. Beyond that point, as density of nodes continues to increase, GPP finds progressively more routes, hovering around 0.1% of failures at 350 nodes. While these failures occur on a tiny fraction of routes in an absolute sense, the nature of the failures is problematic: on a static network, these fractions of destinations are not unreachable temporarily, but *permanently*.

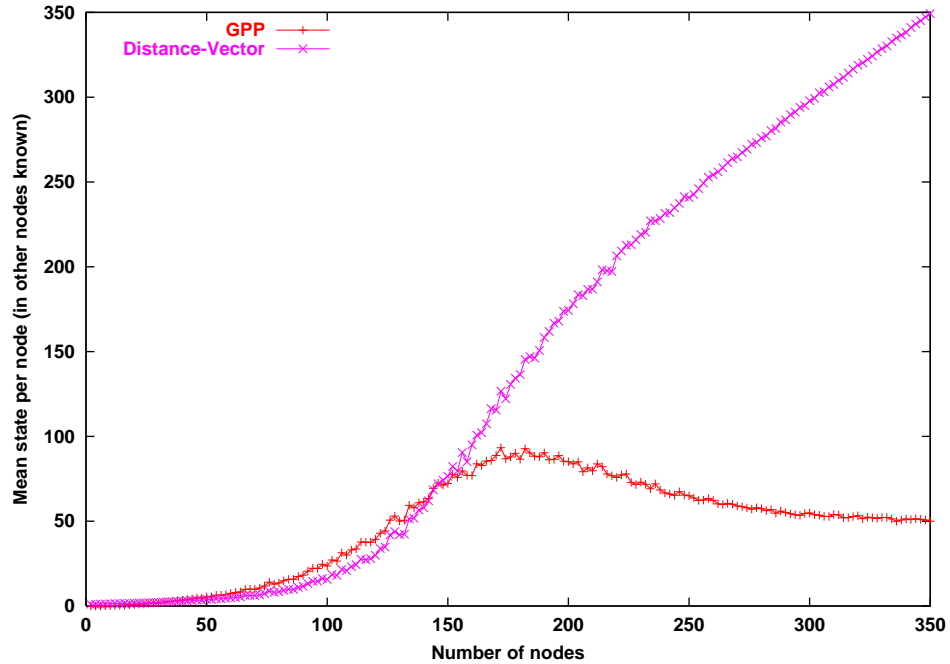


Figure 3.7: State per router, GPP vs. Distance-Vector.

When allowed to converge fully on an idealized network, DV finds all routes; hence it is not shown in Figure 3.6. Note that this 100% success rate of DV applies only to static, idealized networks; it has been shown that DV routing algorithms find significantly smaller fractions of the existing routes on mobile, finite-capacity wireless networks [7].

Figure 3.7 shows that the mean number of nodes a node must keep state for under GPP at first increases with density, reaches a maximum of approximately 100 nodes on networks with approximately 175 nodes, and thereafter *decreases* as density increases, approaching an asymptote of state for 50 nodes. This trend occurs because GPP's state consists of its neighbor table and perimeter lists. At the highest node densities, perimeters are short. When a perimeter includes only immediate neighbors, as is the case on very dense networks, a node need not store a perimeter it learns, as the perimeter offers no additional nodes' positions. It is for this reason that the state each node keeps under GPP on average

levels off as the number of nodes increases. In the middle range of densities measured, perimeters are longer. At the lowest densities measured, perimeters are short because the number of nodes in the network constrains the number of perimeters a node borders and the length of those perimeters. DV routing stores state for a mean number of nodes less than the total number of destinations on the sparsest networks, because so many routes are partitioned on those networks. As density increases, DV routing approaches the expected state size of the number of network destinations. Note that only after density increases enough to connect most of the network graph, at approximately 150 nodes total, does GPP keep less state on average per node than DV, though the two keep similar quantities of state at lower densities. As density increases beyond 150 nodes in the region, GPP stores progressively less state per node relative to DV.

3.2.3 Routing Failures in GPP

We have identified two reasons GPP fails to find routes that exist:

- The no-crossing heuristic removes whichever of two crossing edges in the network graph it reaches second. Removal of this edge may partition the network graph. In these cases, GPP fails to map perimeters that would have crossed the partition.
- Perimeters may not contain a *node* closer to the destination than the point of greedy forwarding failure, but may contain an *edge* containing a point closer to the destination. GPP does not consider such perimeters useful, but they may be.

In Figure 3.8, we see an example of the first type, in which GPP's no-crossing heuristic ignores an edge that effectively partitions the network. Node *S* originates a packet to *D*,

Neighbor	Perimeter Found
a	$S \rightarrow a \rightarrow b \rightarrow S$
b	$S \rightarrow b \rightarrow a \rightarrow S$
c	$S \rightarrow c \rightarrow b \rightarrow S$

Table 3.2: Perimeters found by S in Figure 3.8, one per neighbor.

and the route ($S \rightarrow c \rightarrow d \rightarrow \dots \rightarrow D$) exists. The dotted circle about D is of radius equal to the distance between S and D ($|\overline{SD}|$). The solid lines represent the connectivity graph; these edges represent the links induced by a threshold distance between pairs of nodes. Because S has no neighbor closer to D than itself (note the dotted circle is empty of nodes in range of S), greedy forwarding failure occurs immediately at the packet's originator. For each of its neighbors, a , b , and c , S has mapped one perimeter. These perimeters are listed in Table 3.2. First, note that none of these perimeters are useful to S , because every node on every perimeter S has mapped is a neighbor of S , and thus already available to S for greedy forwarding. All GPP failures share this characteristic: though a route exists, no perimeter containing a closer node is found. In this particular type of failure, the no-crossing rule is directly responsible. The perimeter found via S 's neighbor a cannot include the edge (b, c) because that edge crosses edge (S, a) , taken as the first edge of the perimeter. But it is this edge eliminated by the no-crossing rule that leads to nodes closer to D than S (that is, inside the dotted circle). While the no-crossing heuristic improves reachability overall by forcing perimeter probes to take tours of the boundaries of polygons, it can partition the graph by indiscriminately removing edges in cases such as this one.

The second case in which GPP fails to find routes occurs on topologies *without* any crossing edges. An example appears in Figure 3.9. Here, S originates a packet to D . The

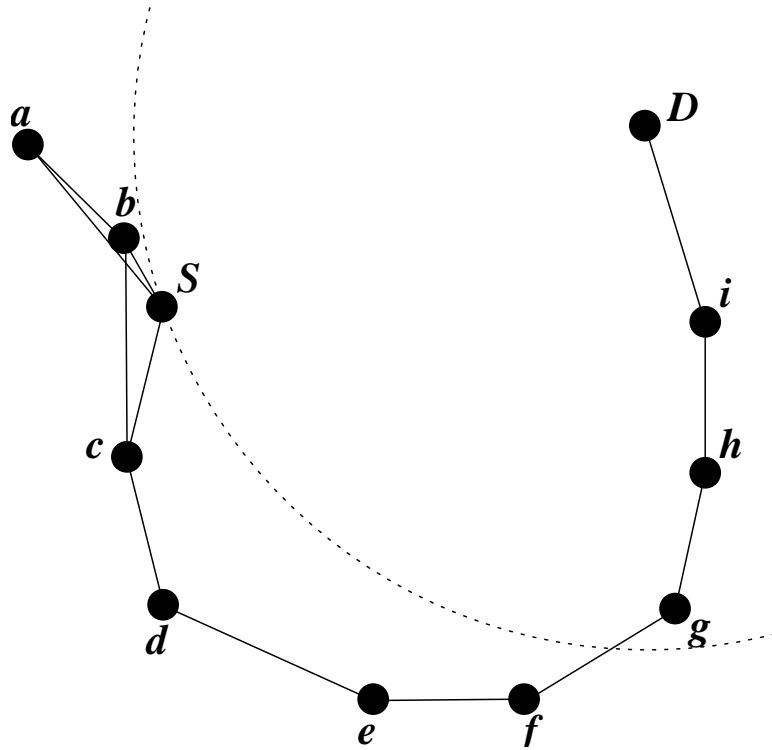


Figure 3.8: Failure of the no-crossing rule: removal of edge (b,c) from S 's perimeter via a partitions the network.

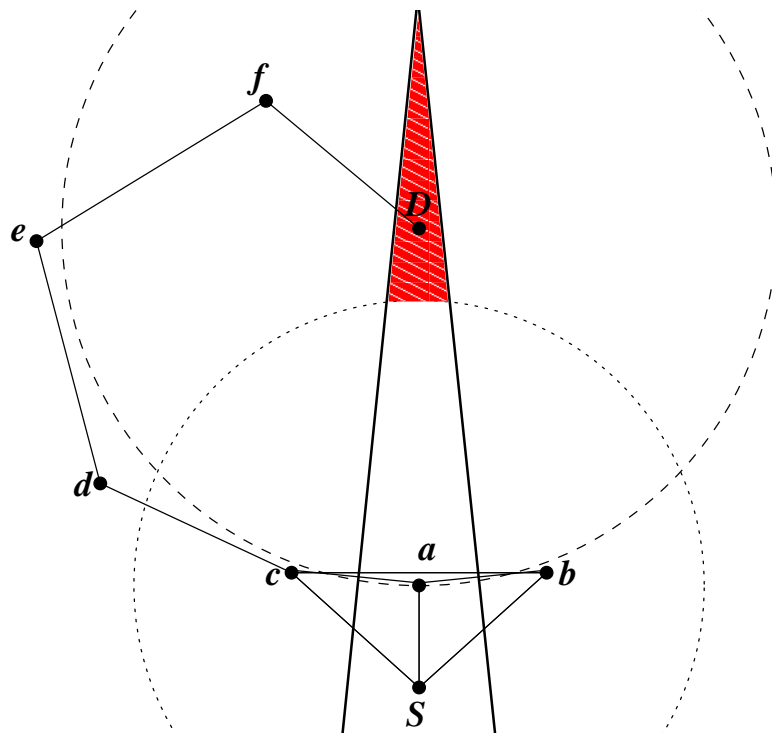


Figure 3.9: Perimeter with no closer node, but with an edge containing a closer point.

Neighbor	Perimeter Found
S	$a \rightarrow S \rightarrow c \rightarrow a$
b	$a \rightarrow b \rightarrow S \rightarrow a$
c	$a \rightarrow c \rightarrow b \rightarrow a$

Table 3.3: Perimeters found by a in Figure 3.9, one per neighbor.

path ($S \rightarrow c \rightarrow d \rightarrow e \rightarrow f \rightarrow D$) clearly exists. Initially, S forwards the packet greedily to a . The dotted circle represents S 's radio range, and the dashed circle is the circle centered at D with radius $|\overline{aD}|$, inside which nodes are closer to D than a . At a , greedy forwarding is impossible (note the empty intersection of the dotted and dashed circles), but a has learned no perimeter containing a node inside the dotted circle, and so GPP drops the packet for D . The perimeters learned by a are shown in Table 3.3. Note that while the perimeter learned by a via c , ($a \rightarrow c \rightarrow b \rightarrow a$), includes edge (c, b) , which includes points closer to the destination D . GPP only examines locations of nodes (vertices), not links (edges). In fact, GPP will fail to forward any packet to a destination in the shaded region that reaches a successfully. The two heavy lines, which are the perpendicular bisectors of edges (c, S) and (b, S) , bound the region a is closer to than both c and b . Eliminating the portion of a 's radio range that overlaps this region leaves the shaded region. Both b and c will forward packets bound for destinations in the shaded region to a greedily, although a has no perimeter to help it forward toward these destinations, and both b and c *do* learn perimeters that will help them forward toward these destinations.

3.3 Planarized Graphs

While measurements taken in simulations show that GPP with the no-crossing heuristic finds the vast majority of routes (over 99.5% of the n^2 routes among n nodes) in randomly generated networks, it is unacceptable for a routing algorithm persistently to fail to find a route to a reachable node in a static, unchanging network topology. Motivated by the insufficiency of GPP's no-crossing heuristic, we present alternative methods for eliminating crossing links from the network.

A graph in which no two edges cross is known as *planar*. As has been done in the idealized simulations presented so far in this thesis, a set of nodes with radios, where all radios have identical, circular radio range r , can be seen as a graph: each node is a vertex, and edge (n, m) exists between nodes n and m if the distance between n and m , $d(n, m) \leq r$. Graphs whose edges are dictated by a threshold distance between vertices are termed *unit graphs*. In the sense that network radio hardware is traditionally viewed as having a nominal open-space range (e.g., 250 meters for 900 MHz DSSS WaveLAN), this model is reasonable. We additionally assume that the nodes in the network have negligible difference in altitude, so that they can be considered roughly in a plane. We discuss these assumptions further in Section 5.3.

The *Relative Neighborhood Graph (RNG)* and *Gabriel Graph (GG)* are two planar graphs long-known in varied disciplines [12], [40]. An algorithm for removing edges from the graph that are not part of the RNG or GG would yield a network with no crossing links. For our application, the algorithm should be run in a distributed fashion by each node in the network, where a node needs information only about the local topology as the algorithm's

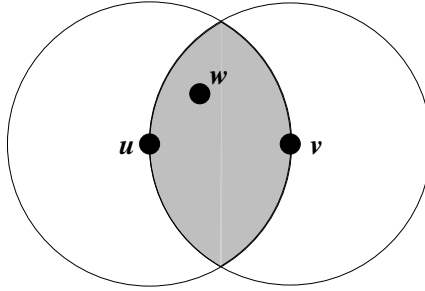


Figure 3.10: The RNG graph. For edge (u, v) to be included, the shaded lune must contain no witness w .

input. However, for this strategy to be successful, one important property must be shown:

Removing edges from the graph to reduce it to the RNG or GG must not disconnect the graph; this would amount to partitioning the network.

Given a collection of vertices with known positions, the RNG is defined as follows:

An edge (u, v) exists between vertices u and v if the distance between them, $d(u, v)$, is less than or equal to the distance between every *other* vertex w , and whichever of u and v is farther from w . In equational form:

$$\forall w \neq u, v : d(u, v) \leq \max[d(u, w), d(v, w)]$$

Figure 3.10 depicts the rule for constructing the RNG. The shaded region, the *lune* between u and v , must be empty of any witness node w for (u, v) to be included in the RNG. The boundary of the lune is the intersection of the circles about u and v of radius $d(u, v)$.

When we begin with a connected unit graph and remove edges not part of the RNG, note that we cannot disconnect the graph. Edge (u, v) is only eliminated from the graph

when there exists a w within range of both u and v . Thus, eliminating an edge requires an alternate path through a witness exist. Each connected component in an unobstructed radio network will not be disconnected by removing edges not in the RNG.

Under the previously described beaconing mechanism, through which all nodes know their immediate neighbors, if u and v can reach one another, they must both know all nodes with the lune. Starting from a full list of its neighbors, N , each node u can remove non-RNG links as follows:

```

for all  $v \in N$  do
  for all  $w \in N$  do
    if  $w == v$  then
      continue
    else if  $d(u, v) > \max[d(u, w), d(v, w)]$  then
      eliminate edge  $(u, v)$ 
      break
    end if
  end for
end for

```

The GG is defined as follows:

An edge (u, v) exists between vertices u and v if no other vertex w is present within the circle whose diameter is \overline{uv} . In equational form:

$$\forall w \neq u, v : d^2(u, v) < [d^2(u, w) + d^2(v, w)]$$

Figure 3.11 depicts the GG graph membership criterion.

As the midpoint of \overline{uv} is the center of the circle with diameter \overline{uv} , a node u can remove its non-GG links from a full neighbor list N thus:

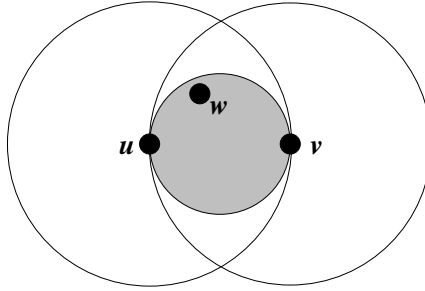


Figure 3.11: The GG graph. For edge (u, v) to be included, the shaded circle must contain no witness w .

```

m = midpoint of  $\overline{uv}$ 
for all  $v \in N$  do
  for all  $w \in N$  do
    if  $w == v$  then
      continue
    else if  $d(m, w) < d(u, m)$  then
      eliminate edge  $(u, v)$ 
      break
    end if
  end for
end for

```

Eliminating edges in the GG cannot disconnect a connected unit graph, for the same reason as was the case for the RNG. Both these algorithms for rendering the graph of the radio network planar take time $O(\text{deg}^2)$ at each node, where deg is the node's degree in the full radio graph.

The RNG is a subset of the GG. This is consistent with the smaller shaded region searched for a witness in the GG, as compared with in the RNG. Figure 3.12 shows a full unit graph corresponding to 200 nodes randomly placed on a 2000-by-2000-meter region, with radio ranges of 250 meters; the GG subset of the full graph; and the RNG subset of the full graph. Note that the RNG and GG offer different densities of connectivity by eliminating different numbers of links. Many MAC layers exhibit drastically reduced efficiency

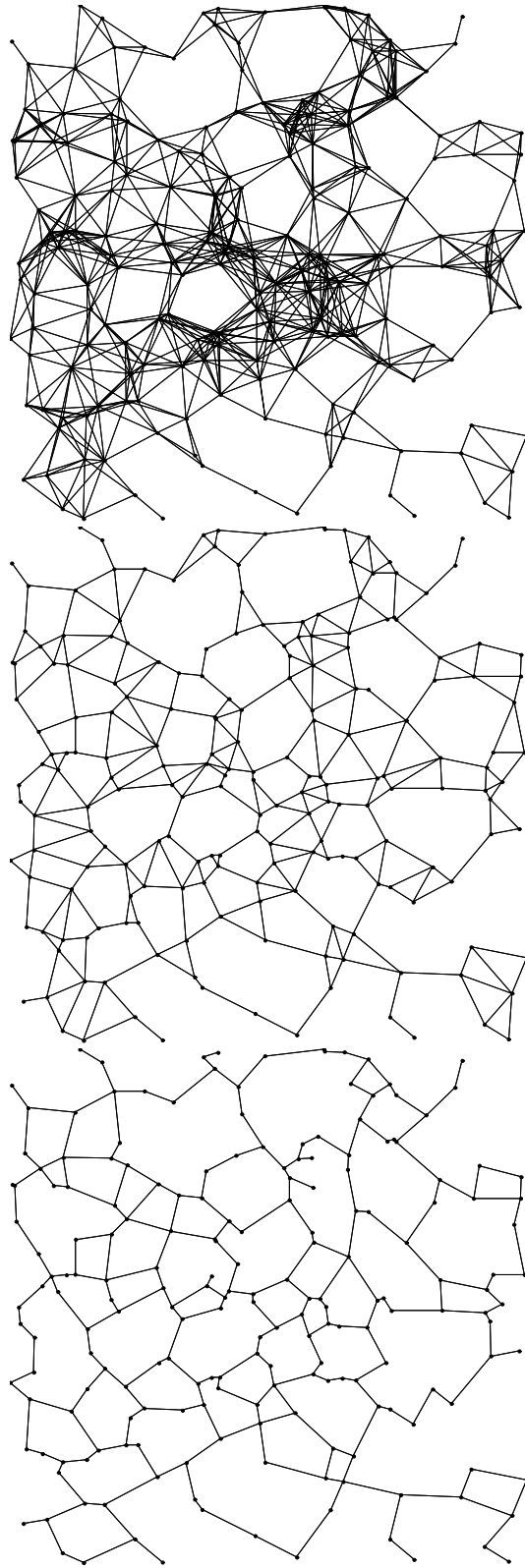


Figure 3.12: Top: the full graph of a radio network. 200 nodes, uniformly randomly placed on a 2000 x 2000 meter region, with a radio range of 250 m. Middle: the GG subset of the full graph. Bottom: the RNG subset of the full and GG graphs.

as the number of mutually reachable sending stations increases [1], [8]. Moreover, while any packet a node transmits monopolizes the shared channel within its radio range, MAC protocols that address the hidden terminal problem, including 802.11 [17], MACA [21], and MACAW [4], deliberately spread contention to the full radio ranges of *both* sender and receiver. On some Frequency Hopping Spread Spectrum MACs, such as Metricom's [3], collisions occur when more than one of a node's neighbors send to it simultaneously. Under such regimes, using fewer links in routing can alleviate contention, and thus increase efficiency.

3.4 GPSR: Combining Greedy and Planar Perimeters

We now present the full Greedy Perimeter Stateless Routing algorithm, which combines greedy forwarding (Section 2.1) on the full network graph with perimeter forwarding on the planarized network graph where greedy forwarding is not possible [23]. Recall that all nodes maintain a neighbor table, which stores the addresses and locations of their single-hop radio neighbors. This table provides all state required for GPSR's forwarding decisions, beyond the state in the packets themselves.

The packet header fields GPSR uses in perimeter-mode forwarding are shown in Table 3.4. GPSR packet headers include a flag field indicating whether the packet is in greedy mode or perimeter mode. All data packets are marked initially at their originators as greedy-mode. Packet sources also include the geographic location of the destination in packets. Only a packet's source sets the location destination field; it is left unchanged as the packet is forwarded through the network.

Field	Function
D	Destination Location
d	Destination Address
h	Previous Hop Address
L_p	Location Packet Entered Perimeter Mode
L_f	Point on \overline{xV} Packet Entered Current Face
e_0	First Edge Traversed on Current Face
M	Packet Mode: Greedy or Perimeter

Table 3.4: GPSR packet header fields used in perimeter mode forwarding.

Upon receiving a greedy-mode packet for forwarding, a node searches its neighbor table for the neighbor geographically closest to the packet’s destination. If this neighbor is closer to the destination, the node forwards the packet to that neighbor. When no neighbor is closer, the node marks the packet into perimeter mode.

GPSR forwards perimeter-mode packets using a simple planar graph traversal. In essence, when a packet enters perimeter mode at node x bound for node D , GPSR forwards it on progressively closer *faces* of the planar graph, each of which is crossed by the line \overline{xD} . A planar graph has two types of faces. *Interior faces* are the closed polygonal regions bounded by the graph’s edges. The *exterior face* is the one unbounded face outside the outer boundary of the graph. On each face, the traversal uses the right-hand rule to reach an edge that crosses line \overline{xD} . At that edge, the traversal moves to the adjacent face crossed by \overline{xD} . See Figure 3.13 for an example. Note that in the figure, each face traversed is pierced by \overline{xD} —the first two and last faces are interior faces, while the third is the exterior face.²

²Forwarding in Figure 3.13 is done in perimeter mode only for exposition; true GPSR forwards greedily when neighbors closer to the destination are available.

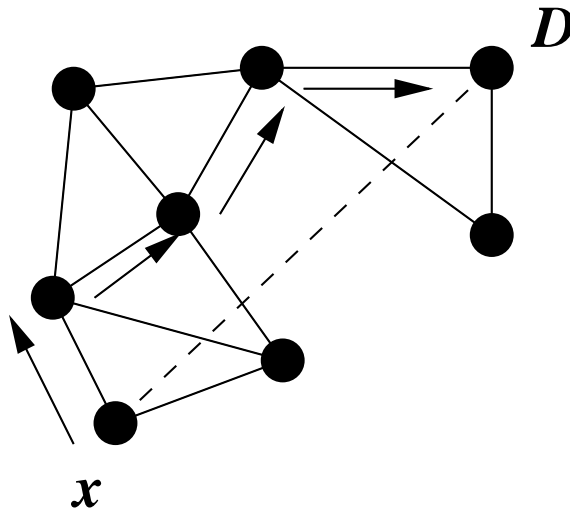


Figure 3.13: Perimeter forwarding example. D is the destination; x is the node where the packet enters perimeter mode; forwarding hops are solid arrows; the line \overline{xD} is dashed.

When a packet enters perimeter mode, GPSR records in the packet the location L_p , the site where greedy forwarding failed. This location is used at subsequent hops to determine whether the packet can be returned to greedy mode. Each time GPSR forwards a packet onto a new face, it records in L_f the point on \overline{xD} shared between the previous and new faces. Note that L_f need not be located at a node; \overline{xD} usually intersects edges, as in Figure 3.13. Finally, GPSR records e_0 , the first edge (sender and receiver addresses) a packet crosses on a new face, in the packet.

Upon receiving a perimeter-mode packet for forwarding, GPSR first compares the location L_p in a perimeter-mode packet with the forwarding node's location. GPSR returns a packet to greedy mode if the distance from the forwarding node to D is less than that from L_p to D .³ Perimeter forwarding is only intended to recover from a local maximum; once the packet reaches a location closer than where greedy forwarding previously failed for that

³GPSR could also return the packet to greedy mode if any *neighbor* were closer to D than L_p . We have not implemented this variant.

packet, the packet can continue greedy progress toward the destination without danger of returning to the prior local maximum.

When a packet enters perimeter mode at x , GPSR forwards it along the face intersected by the line \overline{xD} . Node x forwards the packet to the first edge counterclockwise about x from the line \overline{xD} . This determines the first face over which to forward the packet. Thereafter, GPSR forwards the packet around that face using the right-hand rule. There are two cases to consider: either x and D are connected by the graph, or they are not.

When x and D are connected by the graph, traversing the face bordering x in either direction (we use the previously described right-hand rule) must lead to a point y at which \overline{xD} intersects the far side of the face. This is the case whether the traversed face is interior or exterior. At y , GPSR has clearly reduced the distance between the packet and its destination, in comparison with the packet's start in perimeter mode at x .

While forwarding around a face, GPSR determines whether the edge to the chosen next hop n intersects \overline{xD} . GPSR has the information required to make this determination, as L_p and D are recorded in the packet, and a GPSR node stores its own position and those of its neighbors. If a node borders the edge where this intersection point y lies, GPSR sets the packet's L_f to y . At this point, the packet is forwarded along the *next* face bordering point y that is intersected by \overline{xD} . The node forwards the packet along the first edge of this next face—by the right-hand rule, the next edge counterclockwise about itself from n . This first edge on the new face is recorded in the packet's e_0 field.

This process repeats at successively closer faces to D . At each face, the packet progresses by the right-hand rule until reaching the edge that intersects with \overline{xD} at a point y

closer than the packet's L_f field to D . Finally, the face containing D is reached, and the right-hand-rule leads to D along that face.

When D is not reachable (*i.e.*, it is disconnected from the graph), two cases exist: the disconnected node lies either inside an interior face, or outside the exterior face. GPSR will forward a perimeter-mode packet until the packet reaches the corresponding face. Upon reaching this interior or exterior face, the packet will tour unsuccessfully around the entirety of the face, without finding an edge intersecting \overline{xD} at a point closer to D than L_f . When the packet traverses the first edge it took on this face for the second time, GPSR notices the repetition of forwarding on the edge e_0 stored in the packet, and correctly drops the packet, as the destination is unreachable; the perimeter-mode graph traversal to a reachable destination never sends a packet across the same link in the same direction twice.

Figure 3.14 shows pseudocode for the GPSR forwarding algorithm. Note that we assume throughout this pseudocode that RIGHT-HAND-FORWARD, FACE-CHANGE, and PERI-INIT-FORWARD operate on a pre-planarized graph, with crossing edges already removed; we omit this detail in the pseudocode. GPSR-FORWARD is the top-level forwarding function called for all arriving packets, with arguments p , the packet being forwarded, and n_{in} , the neighbor from which the packet arrived.⁴ If p is a greedy data packet, and greedy forwarding fails, GPSR-FORWARD sets the locations where the packet entered perimeter mode ($p.L_p$) and where the line to the destination intersected the current face ($p.L_f$) to the router's own position. PERI-INIT-FORWARD finds the next router t counterclockwise from the line to the destination, using the same algorithm as RIGHT-HAND-FORWARD. Fi-

⁴If the packet originated at the local node, n_{in} is unused.

```

FACE-CHANGE( $p, t$ )
1   $i = \text{INTERSECT}(t.l, \text{self}.l, p.L_p, D)$ 
2  if  $i \neq \text{NIL}$ 
3    then if  $\text{DISTANCE}(i, D) < \text{DISTANCE}(p.L_f, D)$ 
4      then  $p.L_f = i$ 
5           $t = \text{RIGHT-HAND-FORWARD}(p, t)$ 
6           $t = \text{FACE-CHANGE}(p, t)$ 
7           $p.e_0 = (\text{self}.a, t)$ 
8  return  $t$ 

PERI-INIT-FORWARD( $p$ )
1   $b_{\text{in}} = \text{NORM}(\text{ATAN2}(\text{self}.l.y - p.D.y, \text{self}.l.x - p.D.x))$ 
2   $\delta_{\text{min}} = 3\pi$ 
3  for each  $(a, l)$  in  $N$ 
4  do  $b_a = \text{NORM}(\text{ATAN2}(\text{self}.l.y - l.y, \text{self}.l.x - l.x))$ 
5       $\delta_b = \text{NORM}(b_a - b_{\text{in}})$ 
6      if  $\delta_b < \delta_{\text{min}}$ 
7        then  $\delta_{\text{min}} = \delta_b$ 
8             $a_{\text{min}} = a$ 
9  return  $a_{\text{min}}$ 

GPSR-FORWARD( $p, n_{\text{in}}$ )
1  if  $p.d == \text{self}.a$ 
2    then receive packet
3  else switch
4    case  $p.M == \text{greedy data}$  :
5      if  $\text{GREEDY-FORWARD}(p) == \text{failure}$ 
6        then  $p.M = \text{perimeter data}$ 
7             $p.L_p = p.L_f = \text{self}.l$ 
8             $t = \text{PERI-INIT-FORWARD}(p)$ 
9             $p.e_0 = (\text{self}.a, t)$ 
10           forward  $p$  to  $t$ 
11   case  $p.M == \text{perimeter data}$  :
12     if  $\text{DISTANCE}(\text{self}.l, p.D) < \text{DISTANCE}(p.L_p, p.D)$ 
13       then  $p.M = \text{greedy data}$ 
14            $\text{GREEDY-FORWARD}(p)$ 
15     else  $t = \text{RIGHT-HAND-FORWARD}(p, n_{\text{in}})$ 
16         if  $p.e_0 == (\text{self}.a, t)$ 
17           then drop  $p$ ; destination unreachable
18         else  $t = \text{FACE-CHANGE}(p, t)$ 
19         forward  $p$  to  $t$ 

```

Figure 3.14: Pseudocode for GPSR.

nally, GPSR-FORWARD sets the first edge taken on the perimeter in the packet ($p.e_0$), and forwards the packet to t .

Upon receiving a perimeter-mode packet, GPSR-FORWARD first determines whether the packet has reached a node closer to the destination than the point where it entered perimeter mode; if so, it returns the packet to greedy mode, and forwards it greedily. Otherwise, GPSR-FORWARD calls RIGHT-HAND-FORWARD to determine the next hop router dictated by the right-hand rule. If this next edge is the same as the first edge the packet traversed on the current face ($p.e_0$), the packet has toured the entire face, and the destination is unreachable, so the packet is dropped. If the packet hasn't toured the entire face, GPSR-FORWARD calls FACE-CHANGE to determine whether the packet has reached an edge that crosses the line to the destination. FACE-CHANGE returns the appropriate next hop for the first edge on the next face if such a crossing edge has been reached, or the unchanged next hop found by the right-hand rule if no crossing of the line to the destination is found. Note that changing faces amounts to treating the next hop on the current face as the *previous hop*, and applying the right-hand rule. FACE-CHANGE calls itself recursively, because it is possible that a single node borders *multiple* edges that cross the line to the destination. The recursion terminates upon reaching the edge that crosses the line at the *closest* point to the destination; it must terminate because there is always an edge that crosses the line at a point farther than this closest point.

GPSR will greedily forward a packet to an unreachable destination for potentially many hops before the packet loops on an exterior or interior face and is recognized as undeliverable. If the majority of unreachable destinations lie beyond the boundary of a single face,

undeliverable packets may concentrate at that face of the network graph. This behavior is a direct consequence of GPSR's avoidance of transitive routing protocol traffic across the many hops from a destination to a forwarding router. Other techniques for scaling routing have similar effects, however: the hierarchy used to scale routing on wired networks obscures intra-domain link failures from the backbone in the interest of scaling. Thus, the inter-domain routing system will push a packet a great distance, with the potential result that the packet will be dropped inside the destination AS.

By the end-to-end argument [36], the most logical place for routing unreachability to be determined, and the load on the network from undeliverable packets to be reduced, is at the sending end-system. Mechanisms from inside the network, like ICMP Unreachable, are hard to interpret at senders; it is hard to know on what timescale they indicate unreachability, for example. Applications running over a GPSR-routed network, or any other network, should offer a conforming load; senders should cut their transmission rate absent feedback from receivers.

On a static network, GPSR finds all existing routes (that is, on network graphs where the destination is connected). This fact is clear by inspection: greedy forwarding moves a packet closer to the destination at each hop. Between when a packet enters perimeter mode and leaves perimeter mode, the packet similarly *must* move closer to the destination. If the packet reaches the destination while still in perimeter mode, GPSR clearly finds the route. GPSR only returns a packet to greedy mode from perimeter mode when the packet reaches a point closer to the destination than that where it entered perimeter mode, L_p . If there exists a path to the destination, then the line from the point of entry to perimeter mode to

the destination *must* cut a sequence of adjacent faces on the planarized graph. The right-hand rule visits all edges on a face, until reaching the destination if it is on that face, or the border of the next face cut by the line between L_p and the destination.

Moreover, GPSR never causes a packet to loop forever on a static network. Greedy mode cannot cause a packet to loop, because each greedy hop must move the packet strictly closer to the destination. As stated just above, GPSR never returns a packet to greedy mode from perimeter mode unless the packet has reached a point closer than that where it entered perimeter mode. What remains to be shown is that an invocation of perimeter mode does not loop a packet forever. Perimeter mode traverses a series of adjacent faces, each by the right-hand rule. Because the graph is planar, traversal of a face by the right-hand rule *must* visit each edge on the face. If the destination is connected, there *must* exist a sequence of adjacent faces along the line between L_p and the destination, and the right-hand rule *must* visit the border edge between each pair of these adjacent faces. If the destination is disconnected, then GPSR drops the packet when it visits the first edge taken on a face (e_0) for the second time. Thus, GPSR never loops packets on static networks.

3.5 Robustness and Efficiency on Mobile Networks

To make GPSR robust and efficient on a mobile, wireless IEEE 802.11 network, we made several significant design decisions in and embellishments to the GPSR algorithm.

3.5.1 Use of MAC-Layer Failure Feedback

As done in DSR [7], GPSR receives notification from the 802.11 MAC layer when a packet exceeds its maximum number of retransmit retries. Barring congestive collapse, a retransmit-retry-exceeded failure indicates that the intended recipient has left radio range, either because the recipient failed, or because of motion of the recipient and/or sender. GPSR responds to these notifications by eliminating the destination of the failed packet from its neighbor table. The data packet that elicits such a notification is passed back to the GPSR forwarding logic, for re-forwarding using the newly reduced neighbor table. Use of this feedback often informs GPSR far earlier than otherwise possible through expiration of the neighbor timeout interval (4.5B). This technique allows GPSR nodes to keep more accurate neighbor tables, and therefore make forwarding decisions that more often reflect the current local topology, rather than a stale version of the local topology.

3.5.2 Interface Queue Traversal

Related to MAC-layer feedback, this technique has a profound effect on our results. While an IEEE 802.11 interface repeatedly retransmits the packet at the head of its queue, backing off exponentially between retransmit attempts, it head-of-line blocks, waiting for a link-level acknowledgement from the receiver. This head-of-line blocking reduces the available transmit duty cycle of the interface significantly. For this reason, upon notification of a MAC retransmit retry failure, we traverse the queue of packets for the interface, and remove all packets addressed to the failed transmission's recipient. We pass these packets back to the routing protocol for re-forwarding to a different next hop. This change virtually

eliminated what we'd previously thought to be MAC contention in high-mobility simulations where neighbors were lost frequently; the timeouts and head-of-line blocking were what really had been causing the drops at the interface queue. The implementation of DSR for ns-2 [38] implements this useful optimization, though we don't see it mentioned in the published work on DSR.

3.5.3 Promiscuous Use of the Network Interface

Also as used in DSR [7], GPSR disables MAC address filtering on the IEEE 802.11 radio hardware to receive copies of all packets for all stations within its radio range. As described in Section 2.1, all packets carry their local sender's position, to reduce the rate at which beacon packets must be sent, and to keep positions in neighbor lists maximally current in regions under data traffic load. When a node forwards a data packet, it resets the timer for transmitting the next beacon, since data packets carry beacon-equivalent (address, position) reports. While this technique lengthens data packets by twelve bytes, on shared-medium wireless MACs that use collision avoidance, including IEEE 802.11, the overhead of acquiring the channel for transmitting a packet is much larger than that of lengthening a packet by a dozen bytes. Thus, this optimization also results in use of less of the channel capacity. There is, of course, a power cost in running the IEEE 802.11 radio receive hardware for all packets, regardless of their destination address. But IEEE 802.11 radio hardware implementations expend significantly less power while receiving packets than they do while transmitting packets. We have not performed power consumption measurements of GPSR.

3.5.4 Planarization Triggers

Both the RNG and GG planarizations depend on having current position information for a node's current set of neighbors. We have implemented both planarizations, though the results we present in this thesis use only the RNG. As nodes move, a planarization becomes stale, and less useful for accurate perimeter-mode packet forwarding. In our current implementation, we re-planarize the graph upon every acquisition of a new neighbor, and every loss of a former neighbor, as distinguishable by receipt of a beacon or data packet (promiscuously) from a previously unknown neighbor, and by a beacon timeout for a neighbor, or MAC transmit failure indication. However, this choice will not keep the planarization current if nodes only move *within* a node's radio range, but no nodes move into or out of it. In future, we will incrementally update the planarization upon receipt of every beacon (or promiscuous data packet) from a neighbor, to keep the planarized graph maximally up-to-date.

Chapter 4

Simulation Results and Evaluation

To measure our success in meeting the design goals for GPSR, we simulate the algorithm on a variety of static and mobile network topologies [23]. We focus mainly on the mobile simulation results in this thesis, as that part of the design space is more demanding of a routing protocol—link additions and removals are far more frequent under mobility. To compare the performance of GPSR with prior work in wireless routing, we also simulate Johnson *et al.*'s Dynamic Source Routing, DSR [18], [27], which has been shown to offer higher packet delivery ratios and lower routing protocol overhead than several other ad-hoc routing protocols [7].

4.1 Simulation Environment

We simulated GPSR in ns-2 [39], using the wireless extensions developed at Carnegie Mellon [38]. This simulation environment offers high fidelity, as it includes full simulation of the IEEE 802.11 physical and MAC layers. Moreover, by using the same simulation

code base as the measurement study used to evaluate DSR [7], we ensure our results are directly comparable to those published previously.

The ns-2 wireless simulation model simulates nodes moving in an unobstructed plane. Motion follows the *random waypoint* model [7]: a node chooses a destination uniformly at random in the simulated region, chooses a velocity uniformly at random from a configurable range, and then moves to that destination at the chosen velocity. Upon arriving at the chosen waypoint, the node pauses for a configurable period before repeating the same process. In this model, the pause time acts as a proxy for the degree of mobility in a simulation; longer pause time amounts to more nodes being stationary for more of the simulation.

Our simulations are for networks of 50, 112, and 200 nodes with 802.11 WaveLAN radios, with a nominal 250-meter range. In the simulations where we compare GPSR with DSR, we use simulation parameters identical to a subset of those used by Broch *et al.* [7]; only the number of nodes, in the case of the 112- and 200-node simulations, differs. The nodes are initially placed uniformly at random in a rectangular region. All nodes move according to the random waypoint model, with a velocity chosen uniformly in $[1, 20]$ m/s. We simulate pause times of 0, 30, 60, and 120 seconds, the highest mobility cases, as they are the most demanding of a routing algorithm. Broch *at al.* also simulated 300-, 600-, and 900-second pause times, perhaps in large part because two of the routing algorithms they evaluated (DSDV and TORA) performed well in these cases. We simulate 30 CBR traffic flows, originated by 22 sending nodes. Each CBR flow sends at 2 Kbps, and uses 64-byte packets. The flows are low-bitrate because the IEEE 802.11 MAC is prone to congestion, and these simulations are meant to measure routing protocol behavior, not the

Nodes	Region	Density	CBR Flows
50	1500 m × 300 m	1 node / 9000 m ²	30
112	2250 m × 450 m	1 node / 9000 m ²	30
200	3000 m × 600 m	1 node / 9000 m ²	30
50	1340 m × 1340 m	1 node / 35912 m ²	30

Table 4.1: Simulated Topology Characteristics

limitations of the IEEE 802.11 MAC for data packet capacity. Packets longer than 64 bytes cause fairness problems in the IEEE 802.11 MAC, as longer packets monopolize the channel long enough to cause queue overflow at neighboring nodes, which defer all transmission while the channel is in use. Broch *et al.* simulated a wider range of flow counts (10, 20, and 30 flows); we simulate only the 30-flow case as this case makes the greatest demands on the routing protocols: the most data traffic to forward and most destinations to which to route. Each simulation lasts for 900 seconds of simulated time. We simulate at each pause time with nine different randomly generated motion patterns, and present the mean of each metric over these nine runs. We present confidence intervals for these means. The number of simulations made and their duration is limited by their great expense in computation and storage; *e.g.* the ns-2 wireless MAC layer costs time quadratic in the number of nodes in a simulation for each packet transmittal, because it measures the received signal strength for every transmitted packet at every node in order to determine which nodes receive transmitted packets, and to account for contention at nodes other than the intended receiver. Table 4.1 summarizes the four network types we simulate.

Several parameters govern DSR’s operation. We use the recommended values used in [7], and show those values in Table 4.2. DSR waits 500 ms between retransmits of route

Parameter	Value
Time between route request retransmits	500 ms
Size of source route header	$4n + 4$ bytes
Nonpropagating search timeout	30 ms
Time to hold packets awaiting routes	30 s
Queue size for packets awaiting routes	50 pkts
Maximum gratuitous route reply rate	1/s

Table 4.2: DSR parameters used in simulations.

requests, and backs this value off exponentially when no reply is received for successive route requests. All route requests begin with a single-hop broadcast that propagates no further, as an optimization to reduce routing protocol overhead for the case when a neighboring node has a route to the destination. When DSR has no route for a packet that arrives for forwarding, it is willing to queue the packet for up to 30 seconds to allow a route discovery operation to complete for that packet's destination. Each node is willing to buffer up to 50 such packets at a time. Gratuitous route replies occur when a node sees a packet go by with its own address in a future (as yet untaken) source-route hop; in these cases, the node sends a route reply to the source of the offending packet, to inform the sender of the shorter source route that cuts out the hops *before* itself in the route overheard in the offending packet. DSR will only send a maximum of 1 such gratuitous route reply per second.

These Broch *et al.* simulated networks are quite dense; the y dimension of the space in which nodes are distributed in their 50-node simulations is only 50 meters larger than the simulated radio range. On average, there is one node per 9,000 square meters in these simulations. A radio range is nearly 200,000 square meters. As a result, there are an

average of approximately 20 neighbors within range of the average node in these networks. DSR's caching of overheard routes gives great benefit in such dense topologies. And GPSR can use greedy mode to forward the vast majority of packets.

The last line in Table 4.1 shows a much sparser network configuration that we simulate. In these simulations, the node density is one quarter that in the Broch simulations, and we use a region with a square aspect ratio. The purpose of this last group of measurements is to evaluate the effect of node density on GPSR's performance; recall that greedy forwarding is used less frequently on sparser networks, as shown in Section 2.5.

Our simulations do not include a distributed location database for annotating packets with destinations' positions. Our results here argue that the GPSR approach to routing warrants investigation into efficient location databases, and related work is already underway in this area [25]. In these simulation results, we use an idealized location database: each source annotates packets it originates with the true location of the destination. In this sense, our results represent the lowest control packet load that can be expected from GPSR. Section 5.2 discusses GPSR's interaction with a location database further.

Before gathering the measurement results we present here, we validated the GPSR implementation extensively by running it on hundreds of *non-mobile* topologies, over an ideal MAC layer (the Null MAC [38]), a 2 Mbps, contention-free network. Our goal in these tests is to achieve 100% delivery success to demonstrate that the GPSR code makes correct forwarding decisions. After reaching this 100% goal on the Null MAC, we validated the GPSR implementation on these non-mobile topologies atop the ns 802.11 MAC layer, to verify GPSR's response to MAC transmit failure callbacks.

We evaluate GPSR and DSR using four metrics: packet delivery success rate, routing protocol overhead, optimality of path lengths taken by data packets, and state per router. The first measurements we present are for 50-node topologies and mobility characteristics identical to those simulated in [7], for clearest comparison with prior published results on DSR. Thereafter, we present and discuss measurements on networks with 112 and 200 nodes, and reveal the scaling properties of GPSR and DSR as network diameter increases. Next, we investigate the effect of node density on GPSR’s performance. Finally, we conclude with measurements of the state used on average in each router by GPSR and DSR.

4.2 Packet Delivery Success Rate

Figure 4.1 shows how many application packets GPSR delivers successfully for varying values of B , the beaconing interval, as a function of pause time. The same figure for DSR is included for comparison. All data points are bracketed by their 97.7% confidence interval.¹ Note the narrow range of values on the y axis; all algorithms on this graph deliver over 97% of user packets on average. Only packets for which a path *exists* to the destination are included in the graph; delivery failure to a truly disconnected destination does not represent failure of a routing algorithm. However, as mentioned above, disconnection of a node is extremely rare in these simulations, as connectivity is dense. As one would expect, the decrease in precision of neighbor lists caused by the longer beaconing interval of 3 seconds results in a slightly reduced delivery success rate. But it appears that there is little added

¹The use of 97.7% as the confidence interval is purely to allow use of 2, an easily remembered integer, as the quantile of the unit normal distribution in the confidence interval calculation.

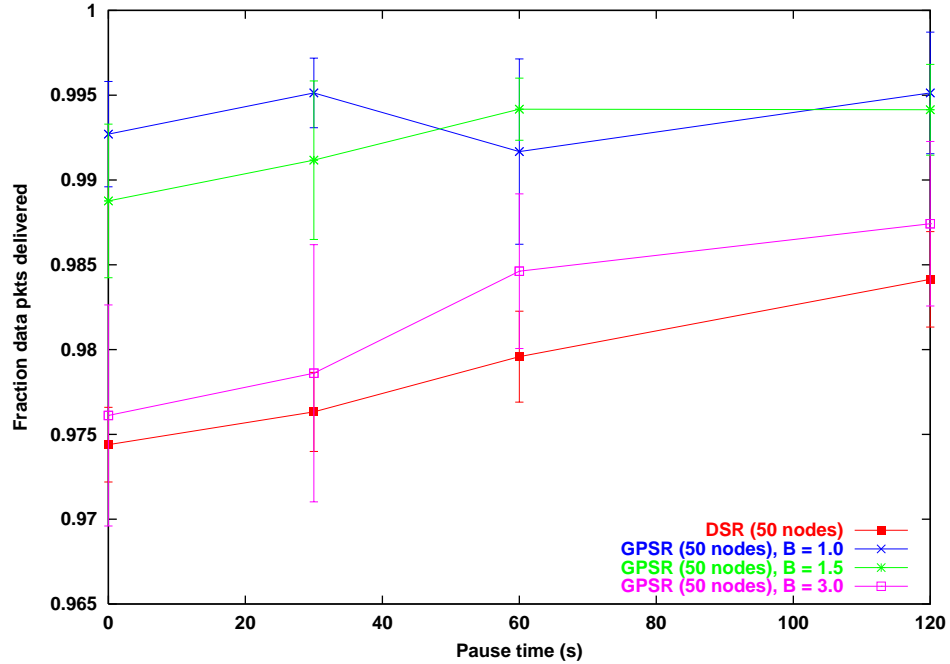


Figure 4.1: Packet Delivery Success Rate. GPSR with varying beacon intervals, B , compared with DSR. 50 nodes.

benefit in decreasing B beyond 1.5 for the simulated mobility rates and radio ranges. At all pause times simulated, GPSR delivers a slightly greater fraction of packets successfully than DSR.

4.3 Routing Protocol Overhead

Figure 4.2 shows the routing protocol overhead, measured in total number of routing protocol packets sent network-wide during the entire simulation, for GPSR with varying B and for DSR. Because GPSR's beacons are sent pro-actively (modulo data traffic with piggy-backed position information), each beaconing interval results in a constant level of routing protocol traffic, independent of pause time (and though we didn't simulate it, number of traffic flows, until application traffic becomes heavy enough to allow nodes never to send

beacon packets). Because DSR is a reactive routing protocol, it generates increased routing protocol traffic as mobility increases. At all simulated levels of mobility, GPSR generates less routing protocol traffic than DSR.

We note with puzzlement that while we believe we run the exact same DSR simulator code as Broch *et al.*, we observe somewhat greater traffic load from DSR than they did in the 30-flow DSR simulations in [7]. To compare with these prior published results, we include a *second* DSR curve, DSR-Broch, in Figure 4.2. Again, our results, both for GPSR and DSR, represent means of nine simulation runs. We see little variance in the individual run results; at these four shortest pause times, there is less simulation sensitivity to the particular random node placement than there is in longer-pause-time simulations. In any event, the contour of their reported curve is the same as that of our DSR curve, and GPSR with $B = 1.5$ offers between a threefold and fourfold overhead reduction under DSR. The contour of the DSR and GPSR curves suggests that as mobility increases further, GPSR may offer greater savings in routing protocol overhead.

4.4 Path Length

Figure 4.3 gives histograms of the number of hops *beyond* the ideal true shortest path length in which GPSR and DSR deliver all successfully delivered packets. The data are presented as percentages of all packets delivered across all nine simulations of GPSR ($B = 1.5$) and DSR, at all simulated pause times. Here, the “0” segment of each bar counts packets delivered in the optimal, true-shortest-path number of hops, and successive bar segments count packets that took one hop longer, two hops longer, &c. The simulator uses the Floyd-

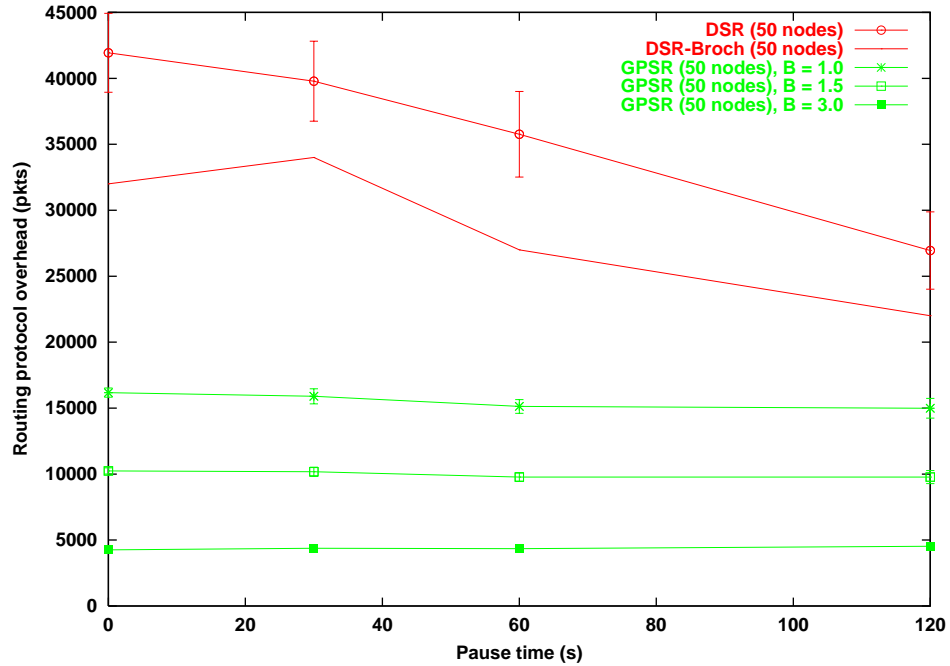


Figure 4.2: Routing Protocol Overhead. Total routing protocol packets sent network-wide during the simulation for GPSR with varying beacon intervals, B , compared with DSR. 50 nodes.

Warshall all-pairs shortest paths algorithm to compute the optimal path lengths between all nodes, and tracks the optimal path lengths as the topology changes under mobility. The simulator must choose an instant at which to decide the optimal path length for each packet. However, packets are not delivered instantaneously, so the optimal path length may lengthen or shorten *during* a packet's journey across the network. The simulator arbitrarily uses the time of a packet's origination as the time when the optimal path length between source and destination is sampled. The optimal path length values are a good approximation of the true values, because the period a packet spends traversing the network (typically, a maximum of tens of milliseconds) is not long enough for the topology to change significantly. Moreover, this sampling method has an inbuilt bias toward *underestimating* the optimal path length. The shortest path length is bounded below by the number of end-

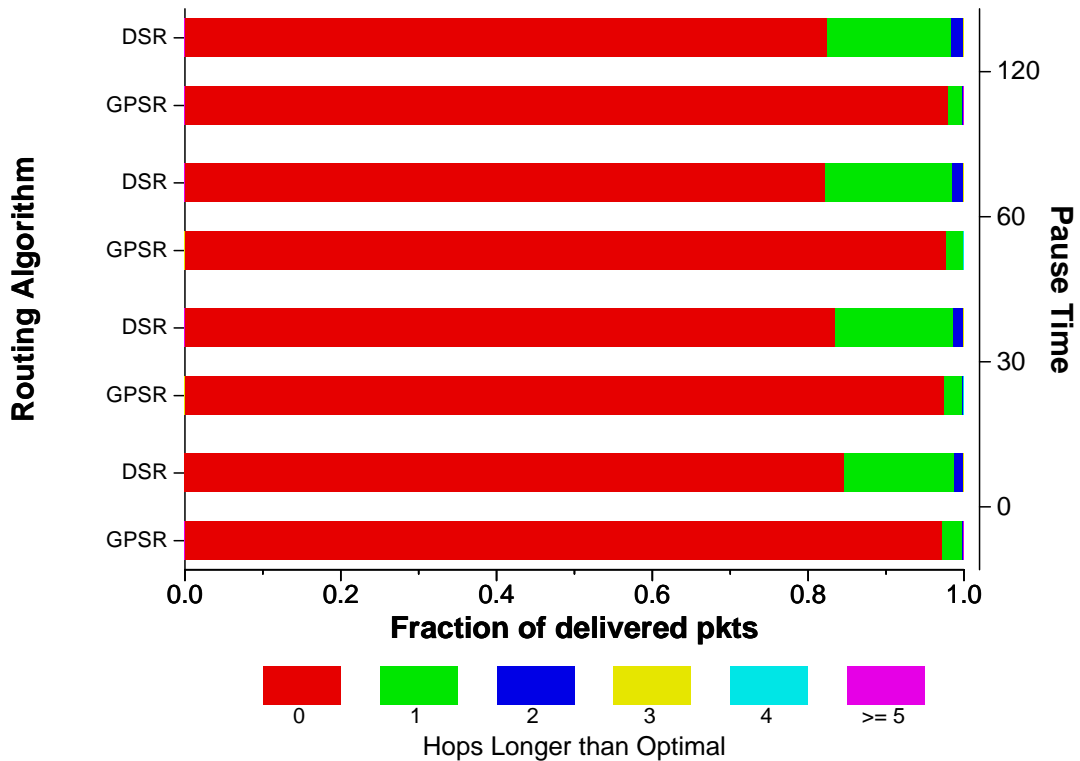


Figure 4.3: Path length beyond optimal for GPSR's and DSR's successfully delivered packets. 50 nodes.

to-end radio ranges that span the Euclidean distance between source and destination; no packet can make the trip in fewer hops. There is no such tight upper bound on the path length, so the distribution of errors should be skewed toward longer-than-accurate during a packet's trip across the network.

GPSR delivers the vast majority of packets in the optimal number of hops. Intuitively, on a dense radio network, greedy forwarding approximates shortest-path routing. GPSR delivers over 97% of its packets along optimal-length paths at all pause times, *vs.* under 85% for DSR at all pause times. This difference is attributable to DSR's caching, which reduces the propagation of route requests, but causes a sub-optimal cached path to be used for forwarding until it breaks.

There is a slight upward trend in the number of packets GPSR delivers in optimal path

length as pause time increases (*i.e.*, as mobility decreases). When a new neighbor moves in range of a forwarding router in such a way that a new shortest possible path is formed, whether or not the new shorter route is used depends on whether the forwarding GPSR node learns of the new node's arrival within its radio range by the time a packet arrives for forwarding. As mobility decreases, the average length of time a new neighbor that allows a new shortest path has been in range increases, and GPSR is more likely to have heard a beacon or data packet from the new neighbor that allows a new shortest path. This trend makes intuitive sense: as the topology varies more slowly, there is a greater chance GPSR's pro-active beaconing has had time to describe the new topology.

There is a slight *downward* trend in the number of packets DSR delivers in optimal path length as pause time increases. This trend occurs because DSR generally uses a route until that route breaks; even if a shorter route comes into existence, DSR won't discover it until forced to flood a new route request. When mobility decreases, routes break less frequently, and DSR is slower to learn new, more optimal paths. This trend is a bit counterintuitive: one might expect reduced mobility to make routing easier, and therefore to yield more frequent use of the shortest path. It is the reactive nature of DSR that is responsible: DSR's design prioritizes avoidance of flooded routing protocol traffic above discovery of true shortest-path routes, but below avoidance of network partition for a destination.

4.5 Effect of Network Diameter

Figures 4.4, 4.5, 4.6, and 4.7 present packet delivery ratio and overhead results for larger-scale, 112- and 200-node networks with identical traffic sources and node density. Again,

all results represent the mean and 97.7% confidence intervals across 9 simulations. In these measurements, the regions on which nodes move are 2250 by 450 meters and 3000 by 600 meters, respectively, such that the number of square meters per node ($9000 \text{ m}^2/\text{node}$) remains the same as that in the 50-node simulations. The intent in these simulations is to evaluate the scaling of DSR and GPSR as network diameter increases. When routes are longer, the probability of a route's breaking increases. The traffic sources are the same as in the smaller network simulations: 30 CBR sources of 2 Kbps each, transmitting 64-byte packets. We do not increase the number of flows despite the increased number of nodes in the network because DSR generates routing protocol packets reactively, and we seek to measure DSR's behavior *only* on networks of wider diameter, not under workloads with more destinations.

Note that in Figure 4.7, the y axis is log-scaled. For each number of nodes, GPSR's traffic overhead once again remains flat, as it is a non-reactive protocol. At a constant node density, network diameter has no effect on GPSR's *local* routing protocol message traffic, since GPSR never sends routing packets beyond a single hop. This particular metric, *network-wide* count of routing protocol packets, shows the GPSR beacon traffic to be linear in node count, as compared with the 50-node simulations. DSR's traffic overhead is significantly larger on the wider-diameter, 112- and 200-node networks, as the protocol must propagate source route information along the full length of a route, and longer routes break more frequently. DSR's caching of routes does not avoid this significant message complexity increase. Note that comparing total numbers of routing protocol packets across the entire network for varying number of nodes unfairly penalizes GPSR, in the sense that

GPSR generates a uniform routing protocol traffic distribution across nodes, because it is purely pro-active and generates beacons at a fixed rate (modulo piggybacked position information on data packets). Because wireless network capacity increases with the spatial diversity of transmitters, GPSR's beacons offer the same *local* network load so long as the *density* of nodes remains fixed. In contrast, DSR's routing protocol overhead is decidedly non-linear in the number of nodes, such that the local network load caused by routing protocol packets clearly increases significantly in the number of nodes.

GPSR's traffic delivery ratio remains high at all pause times on these larger-scale networks. It is GPSR's use of only local topology information that allows the protocol to maintain this delivery ratio; there is little penalty for GPSR as the path length from source to destination lengthens. Moreover, GPSR recovers from loss of a neighbor by greedily forwarding to another appropriate neighbor; this failover is instantaneous. DSR's delivery ratio decreases considerably in the wider-diameter network, owing to DSR's need to maintain full, end-to-end source routes, and re-query them increasingly frequently as diameter and mobility increase.

Note that the maximum shortest path lengths between nodes in these wider-diameter simulations are still under 16 nodes. We mention this fact as the DSR simulator code uses a compile-time constant for the maximum length of a route it will discover, and maximum propagation distance for route requests.

In these 112- and 200-node runs, DSR's 64-route cache is full at virtually every node. While the number of destinations in the network is only 30 in our simulations, DSR caches multiple routes per destination, and might profit from being able to cache more routes,

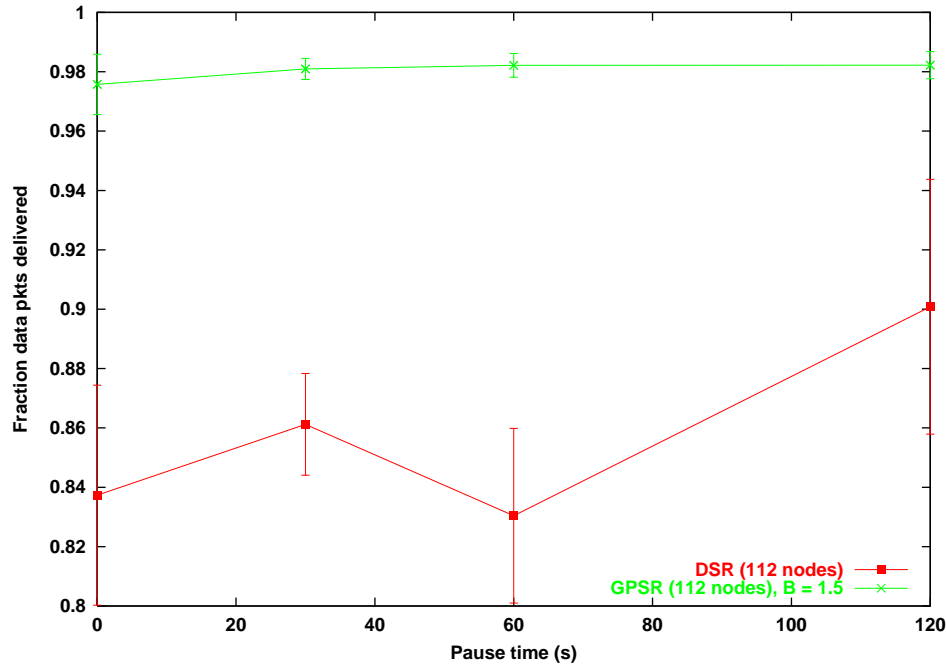


Figure 4.4: Packet Delivery Success Rate. For GPSR with $B = 1.5$ compared with DSR. 112 nodes.

though at the expense of increased per-router state (see the next section).

Figures 4.8 and 4.9 show path length histograms for 112- and 200-node networks across all pause times for DSR and GPSR, as presented before for 50-node networks. Here again, as was the case in the 50-node path length data, GPSR consistently finds shorter paths for a greater fraction of packets than DSR. However, as the network diameter increases, both GPSR and DSR deliver fewer packets in the optimal path length. In the case of GPSR, the longer the shortest path between two nodes, the greater the chance that the path includes a node which has just arrived in range of its predecessor, and isn't yet known to the predecessor at the time the packet reaches the predecessor, resulting in a longer-than-optimal path.² Similarly, the longer a path between two nodes is, the greater the chance

²Of course, GPSR will always learn if the shortest path has become *longer*, because this situation corresponds to loss of a neighbor, which will be indicated by a MAC layer retransmission retry failure for that neighbor.

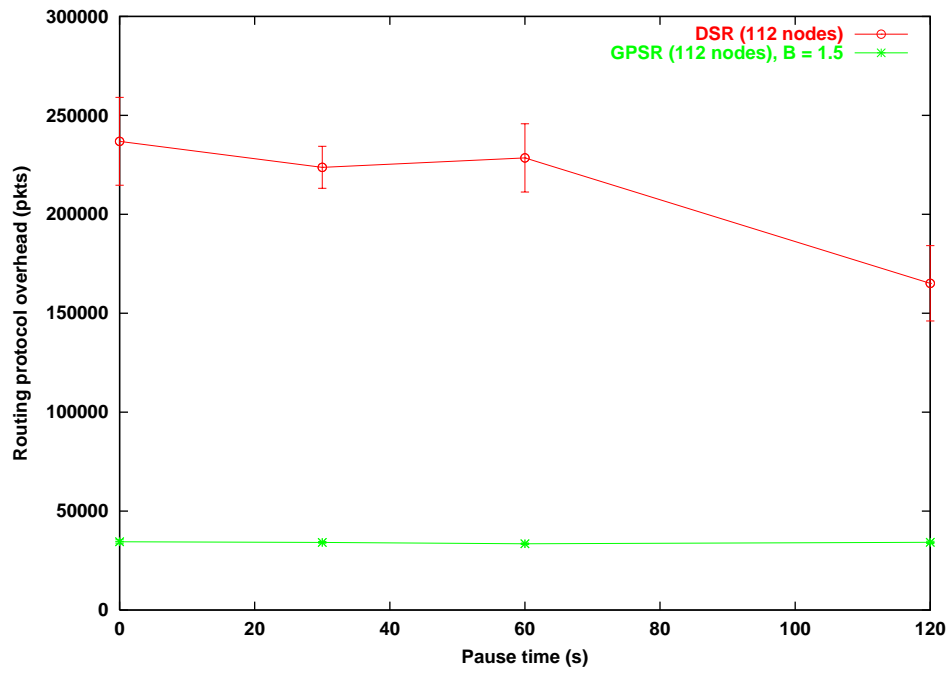


Figure 4.5: Routing Protocol Overhead. Total routing protocol packets sent network-wide during the simulation for GPSR with $B = 1.5$ compared with DSR. 112 nodes.

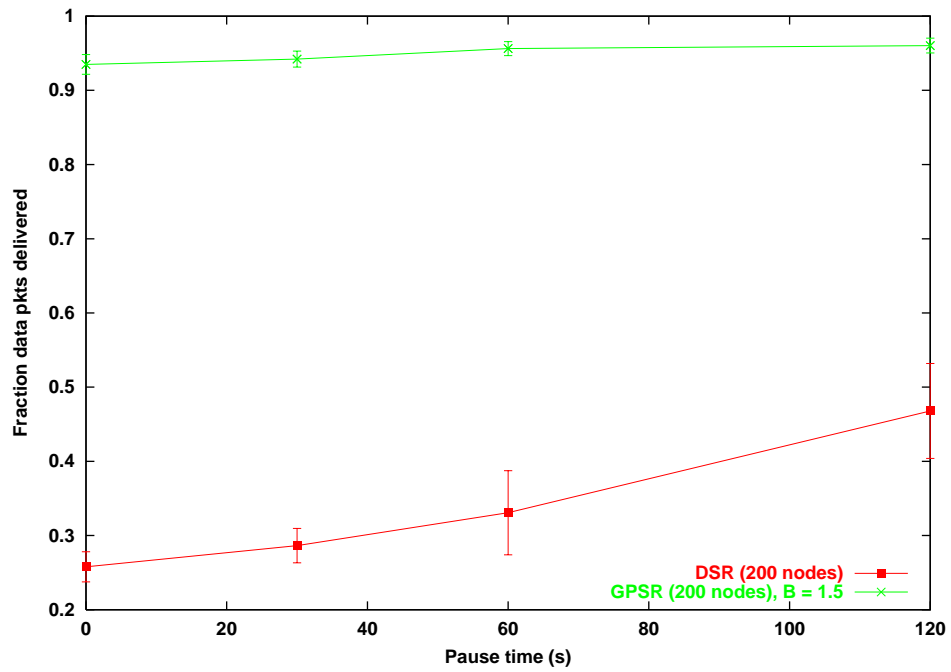


Figure 4.6: Packet Delivery Success Rate. For GPSR with $B = 1.5$ compared with DSR. 200 nodes.

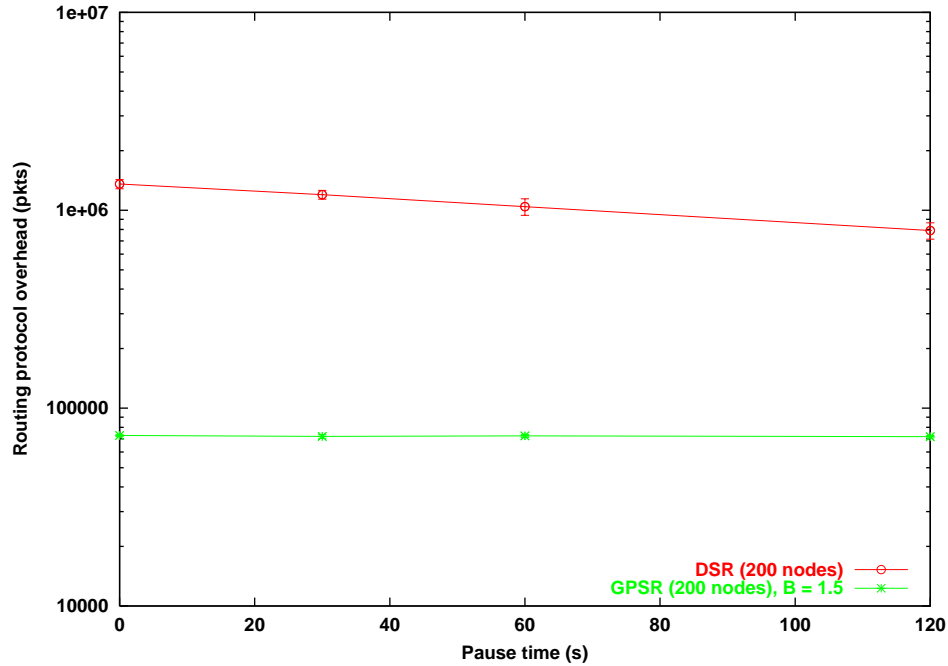


Figure 4.7: Routing Protocol Overhead. Total routing protocol packets sent network-wide during the simulation for GPSR with $B = 1.5$ compared with DSR. y axis log-scaled. 200 nodes.

that a shorter alternative exists for a portion of the path, but DSR learns new shortest paths when a path breaks altogether.

GPSR again delivers more packets along the optimal path as mobility decreases in these larger-scale networks. DSR also shows the same downward trend in the number of packets delivered along the optimal path, as mobility decreases.

4.6 Effect of Node Density

In Figures 4.10, 4.11, and 4.12, we provide measurements of GPSR and DSR running on a 50-node network deployed over a 1340-by-1340-meter region. In this section, these results are averaged over four simulations. The lower density of nodes, one quarter that in the

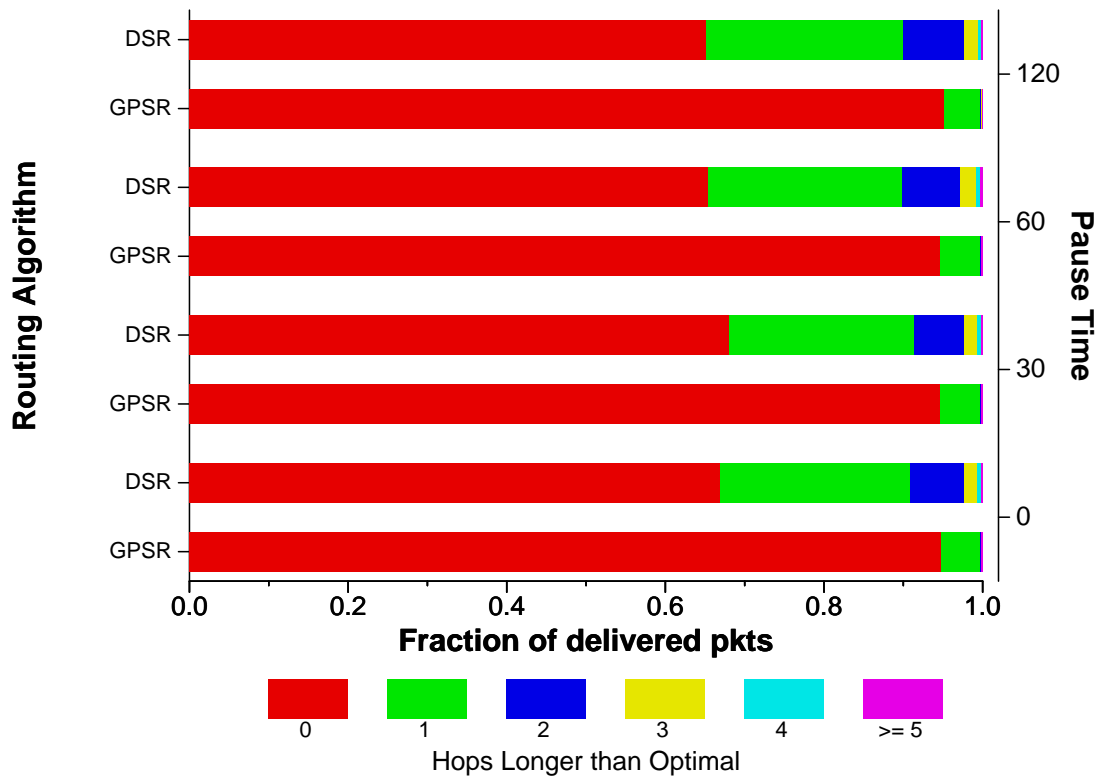


Figure 4.8: Path length beyond optimal for GPSR's and DSR's successfully delivered packets. 112 nodes.

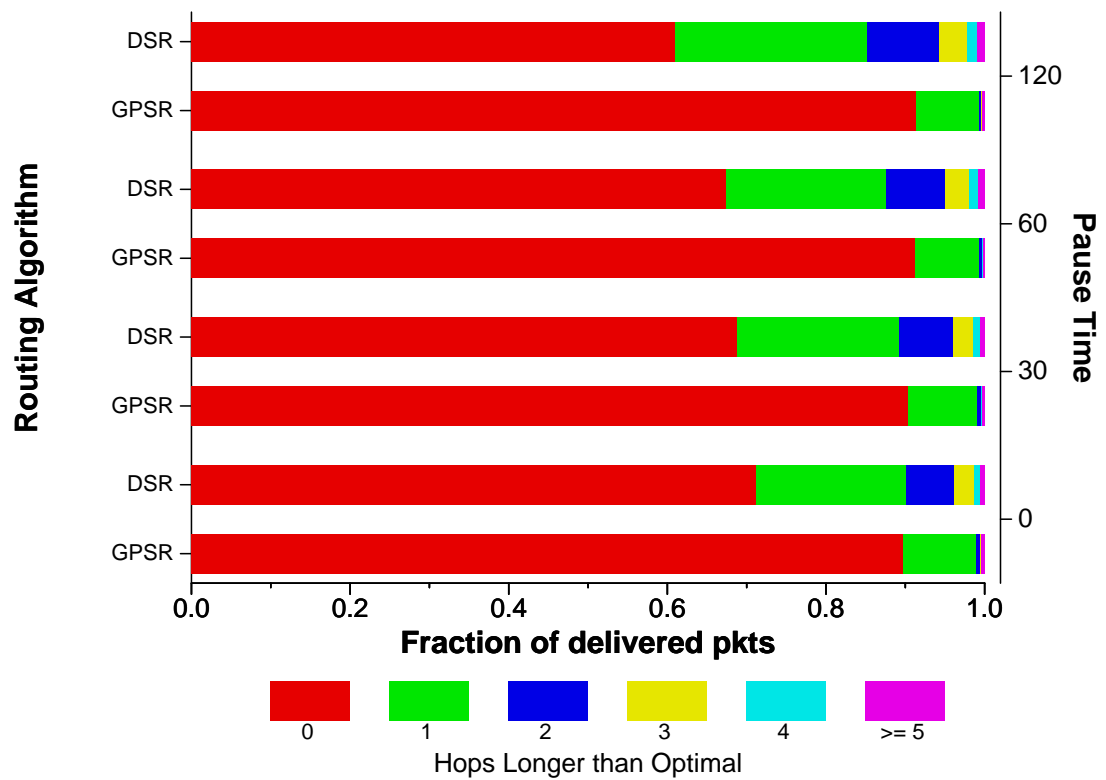


Figure 4.9: Path length beyond optimal for GPSR's and DSR's successfully delivered packets. 200 nodes.

preceding simulations, causes voids to occur more frequently on average, and thus forces GPSR to forward packets in perimeter mode more often.

It is important to note that as shown in Section 2.5, as networks become more sparse, two effects are observed: voids occur along more routes *and* more destinations are disconnected. The presence of more disconnected nodes affects both GPSR and DSR, in that both routing algorithms incur a cost when attempting to route to an unreachable destination. DSR will flood a query, potentially learn a stale cached route, and requery, until finally no stale cached routes remain in the network, and no reply for the last query returns. At this point, DSR backs off exponentially on subsequent queries for the same destination. When GPSR attempts to route a packet to a disconnected destination, the packet will tour the face that encloses that destination, and be dropped when it traverses that face's first edge for the second time. This, too, represents a cost; the tour of the last face consumes network bandwidth for an undeliverable packet. As discussed in Section 3.4, properly engineered traffic sources are responsible for end-to-end detection of disconnected destinations, and backing off their transmit rates accordingly. We must use non-deferential, CBR sources to make comparison of routing algorithms possible; if the sources backed off in response to failure of a routing algorithm to deliver packets, the relative meaning of different algorithms' packet delivery ratios and routing protocol overhead statistics would be unclear. In the simulations presented thus far, nearly all destinations are reachable all the time. In this set of simulations on sparser networks, however, we used 1 Kbps CBR sources, to ensure neither DSR nor GPSR would congest the IEEE 802.11 network because of the additional

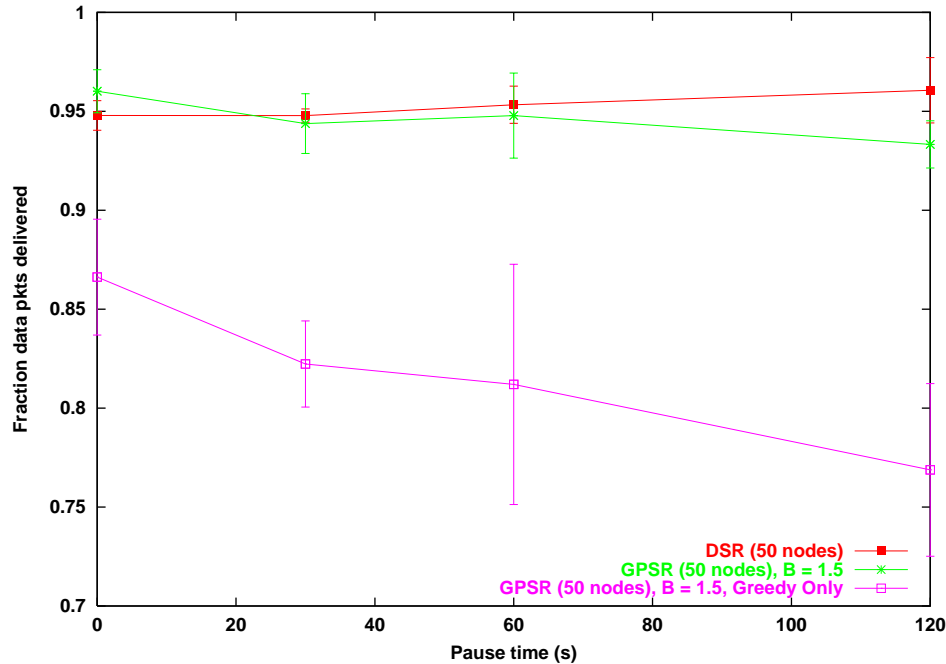


Figure 4.10: Packet Delivery Success Rate. For GPSR with $B = 1.5$ compared with DSR. 50 nodes, sparse topology.

cost of packets for unreachable destinations.³

Figure 4.10 shows that GPSR successfully delivers roughly the same percentage of packets as DSR across all pause times on these sparser networks. The curve labeled “greedy only,” new to this plot, shows the percentage of packets that were delivered using *only* greedy mode. Thus, the gap between the greedy-only curve and the GPSR curve shows clearly the importance of perimeter mode in the robustness of GPSR on sparser networks. The downward trend in the greedy-only curve is unexpected; the trend suggests that perimeter mode is used more often at longer pause times, and thus that networks whose nodes pause for longer tend to be sparser than those whose nodes pause for briefer periods. This analysis is correct, and the random waypoint model is the cause of this phenomenon. Nodes moving

³On properly engineered networks, CBR and other sources would be deferential, either natively in the sources themselves, or as enforced by an acknowledgement protocol in a layer beneath the sending application. DSR’s route replies and route errors play the role of acknowledgements in this way.

under the random waypoint model are in one of two states: moving, or paused. Because destinations are chosen uniformly at random, a paused node is equally likely to be toward the periphery of the simulated region or toward the center of it. However, moving nodes are *more likely to be toward the center of the region*, because on average, a node moving from one uniformly randomly selected position to another will tend to cross the center of the region rather than remain in the outer periphery of the region. Thus, the greater the fraction of nodes that are in the moving state, the more clustered the topology is toward the center of the region, and the greater the fraction of nodes that are paused, the more relatively dispersed the nodes are. We verified this effect empirically by measuring the number of nodes in the circle of diameter 670 meters, centered in the 1340-by-1340-meter region, over time, for each pause time. This property of the random waypoint model may mirror reality in some applications, in the sense that in a metropolitan area, mobile users may tend to cross the center of the area during the work day, but be more dispersed on average while stationary in the evening.

Figure 4.11 reveals that GPSR exhibits lower routing protocol overhead than DSR on these sparser networks. The number of packets sent for disconnected destinations is responsible for DSR's increased routing protocol overhead beyond that in the dense 50-node simulations. Moreover, DSR's caching is likely less effective in sparser topologies than in denser ones, because nodes promiscuously overhear source routes less often.

Figure 4.12 shows the cost GPSR pays on sparse networks: non-shortest-path packet delivery. In these simulations, GPSR delivers more packets along longer-than-optimal routes than in the ones of denser networks. While GPSR still delivers more packets than

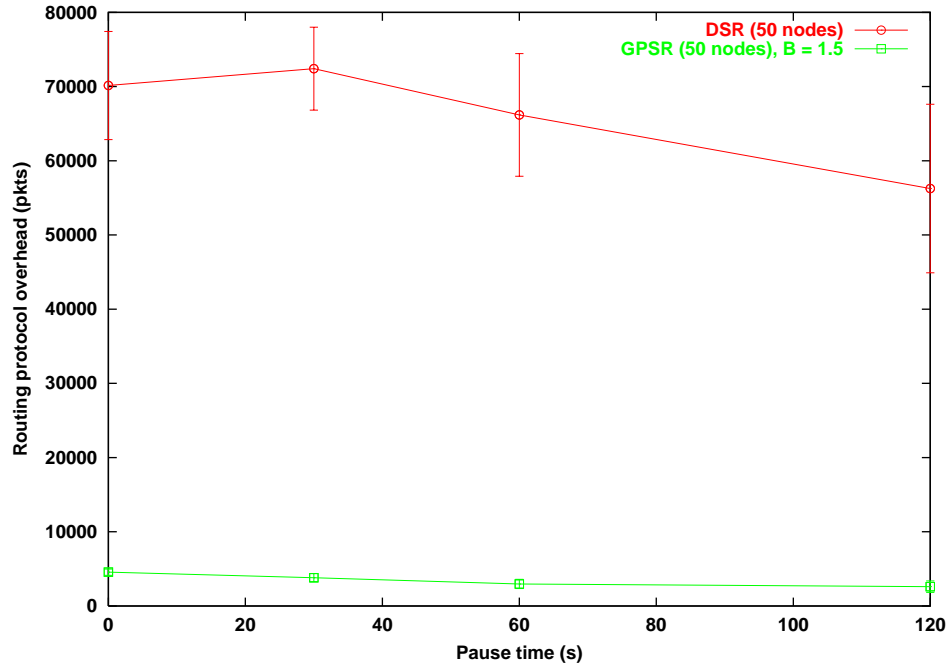


Figure 4.11: Routing Protocol Overhead. Total routing protocol packets sent network-wide during the simulation for GPSR with $B = 1.5$ compared with DSR. 50 nodes, sparse topology.

DSR in the optimal path length across all simulated pause times, the fraction of packets for which GPSR does so decreases as pause time increases, reflecting the random waypoint model's sparser topologies in these cases, and the non-shortest-path nature of perimeters. For GPSR, the tail of the distribution, contained in the " ≥ 5 " bin, is significantly heavier than it is for DSR in these simulations, and includes a tiny fraction ($< 0.5\%$) of packets that take more than 50 hops longer than the shortest path to reach the destination. These packets experience such long paths because they loop temporarily while perimeters change on a dynamic network; this effect is discussed further in Section 5.1.

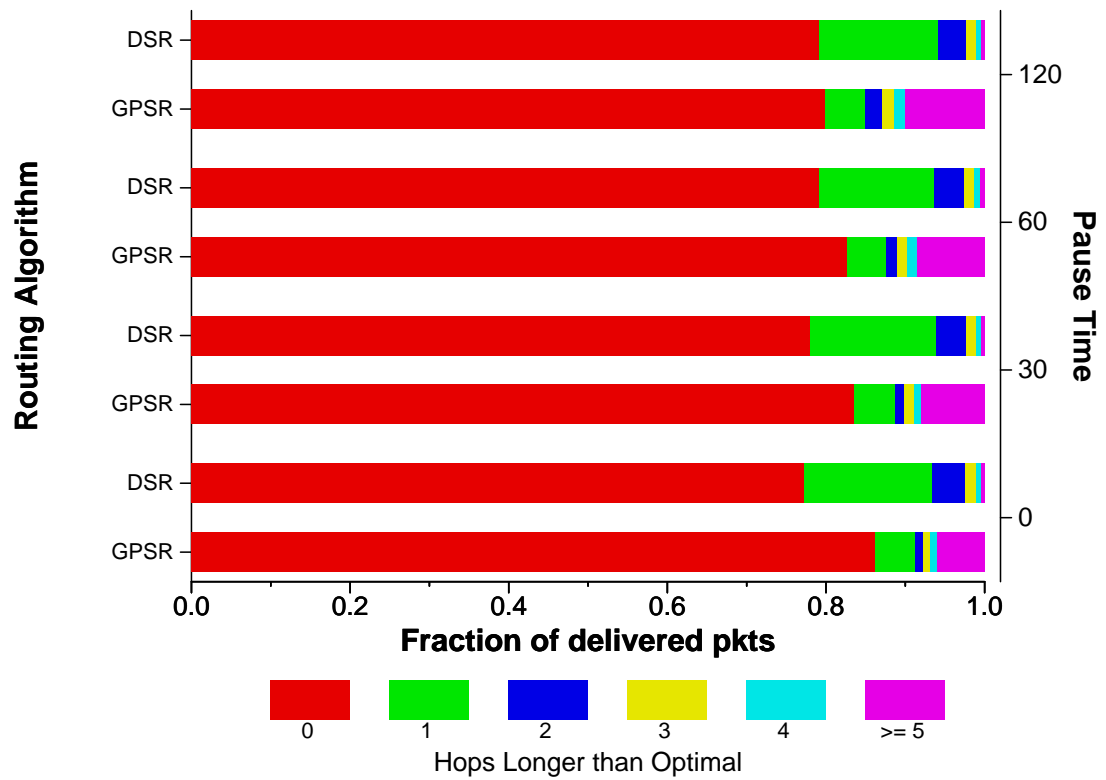


Figure 4.12: Path length beyond optimal for GPSR's and DSR's successfully delivered packets. 50 nodes, sparse topology.

4.7 State per Router

When measuring state per router, the relevant metric is the number of *nodes* in a router's tables—not the number of routes. Because DSR uses source routes, each route stored by a DSR router requires storage for each node along the route.

We measure both GPSR's and DSR's average per-node state for the set of 200-node simulations with pause time 0. Because the state maintained by a node in these networks changes constantly, we take a snapshot at time 300.0 seconds in each of our 900-second simulations, and measure the state in use by each node at that instant. A GPSR node stores state for 26 nodes on average in the pause-time-0, 200-node simulations. This figure depends on node density, as the only state a GPSR router keeps is an entry for each of its single-hop radio neighbors. Note that as number of nodes and network diameter increase in the 50-, 112-, and 200-node simulations, GPSR stores the same quantity of state, as the density of nodes remains fixed.

In comparison, the average DSR node in our 200-node, pause-time-0 simulation stores state for 266 nodes—more than the total number of destinations in the network. It should be noted that this value for DSR is clamped by the fixed-size route cache in the DSR simulator's implementation; this cache is limited to 64 routes. While DSR might profit in robustness from a larger route cache, the state cost per node will increase dramatically as the network size increases, and increasingly many more diverse routes are discovered. A larger DSR route cache will also store more broken routes, as mobility and network diameter increase. Figure 4.13 compares the state size stored on average by DSR and GPSR, in both nodes and bytes.

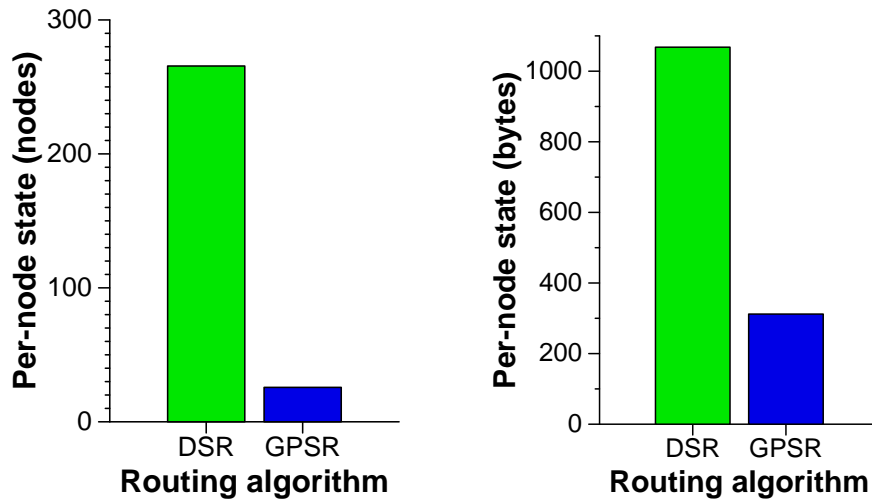


Figure 4.13: Average state size stored, 200-node, pause-time-0 simulations, DSR vs. GPSR. Left: nodes stored; right: bytes stored.

When routes are longer in hops, DSR will store more state at each router. Thus, DSR stores state proportional to the network diameter. A DSR router also will store routes for all destinations for which packets arrive, so DSR also stores state proportional to the number of destinations in a traffic workload.

Each node stored in a GPSR router’s neighbor table arguably requires more storage than a node stored in a DSR router’s table, as GPSR routers must track the positions and addresses of their neighbors, while DSR routers need only track the addresses of hops in a source route. GPSR uses 12 bytes for each neighbor in its table; two 4-byte floating point values for position coordinates, and 4 bytes for address. DSR uses 4 bytes per address. However, this is a constant factor difference, dominated asymptotically by the number of nodes stored.

Chapter 5

Discussion and Future Work

In this chapter, we describe the characteristics of networks where we expect GPSR to work best and worst; discuss system design choices for GPSR networks; and suggest future directions for extending and enhancing GPSR.

5.1 GPSR's Properties

The mobile simulation results presented in Chapter 4 show that GPSR remains robust on networks of increasing diameter and node count, while continuing to exhibit small routing protocol overhead. The simulated networks were all of equal density to those simulated by Broch *et al.* in [7]. The density of these networks has an important implication for GPSR: it means that greedy forwarding can be used for the vast majority of packet forwarding decisions. This relationship between density and the success of greedy forwarding alone was shown in Chapter 2. Greedy forwarding approximates shortest paths well on these dense networks, and its use of only local topological information allows it to recover quickly from

the loss of a neighbor, and benefit quickly from the acquisition of a neighbor.

On sparser networks, perimeter mode will be used more frequently. Packets that use perimeter mode tend to be delivered in longer than the shortest-path number of hops for two reasons. First, a packet may greedily traverse hops that take it on a “blind alley” toward the destination, that must effectively be retraced in perimeter mode. Second, perimeter mode, is by nature circuitous in the paths it traces around planar faces, which only use a subset of the full radio graph’s edges.

In addition, perimeters are less robust than greedy forwarding under mobility. While a packet tours the interior of a planar face, the topology can change such that an inner face, that shares its boundary with the outer face the packet was touring, but is narrower in diameter than the outer face, closes around the packet. This inner face may not cross the line between the packet’s point of entry into perimeter mode and the packet’s destination. If it does not, the packet will endlessly loop around the inner face, until the inner face reopens or moves to cross the line to the destination, or until the packet is dropped when its time-to-live maximum hop counter reaches zero. An example of this phenomenon appears in Figure 5.1. Here, S sends a packet to D , and while the packet traverses the perimeter of the large void by the right-hand rule, node x moves such that the two dashed edges are newly created. Because the new inner perimeter involving x does not cross the line from the point of entry into perimeter mode to D , the packet will loop on the inner perimeter until its TTL is decremented to zero. Note that the first edge of the outer perimeter recorded in the packet by GPSR is not useful in detecting this inner loop.

It is important to note that the described inner-face phenomenon occurs less frequently

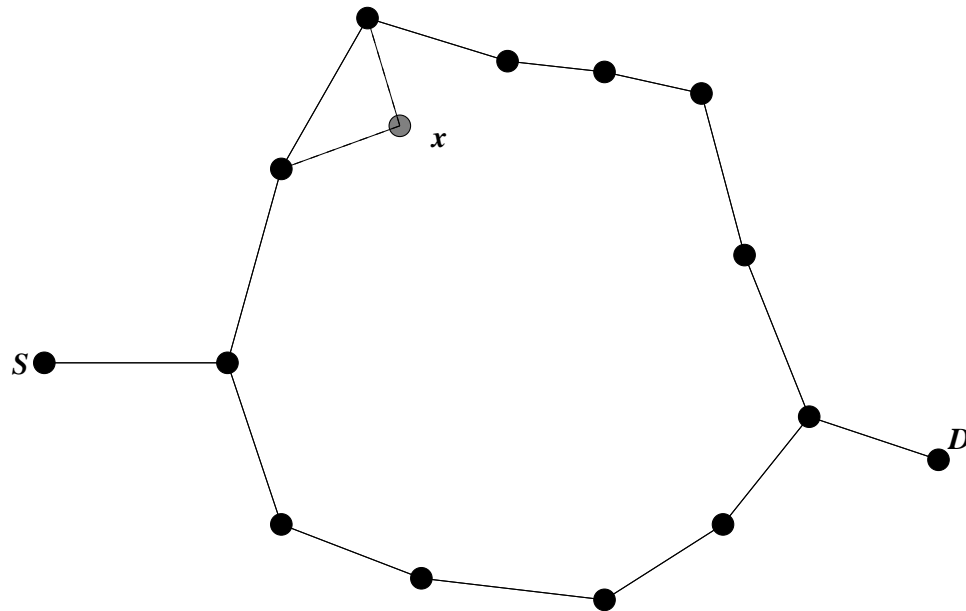


Figure 5.1: An inner perimeter closing around a packet.

as density decreases; the closing of an inner face requires nodes to be placed to form an entire face within the outer one. This relationship is virtuous, in that perimeters are used for forwarding more often as density decreases. Perimeter mode is sufficiently robust on sparse, mobile networks to contribute significantly to the percentage of packets delivered successfully by GPSR, as shown in the sparse network results in the previous chapter.

Few routing protocols are loop-free on dynamic topologies. The small class that trade off routing protocol overhead for loop freedom—they send protocol messages in an attempt to force consistency on the routes chosen at nodes. If the topology changes more quickly than they respond, these protocols suffer unreachability of destinations. This phenomenon is clearly demonstrated in [7]: the DSDV protocol uses sequence numbers to force consistency on routes. When the protocol doesn't aggressively push sequence number changes (caused by route changes) throughout the network, it fails to route to many destinations. When it does push sequence number changes aggressively, it generates large

routing protocol overhead. DSR is immune to looping traffic, because it uses source routes, which can be constructed so as not to contain cycles. However, it suffers similarly as DSDV does under mobility: as shown in Chapter 4, DSR must generate large volumes of routing protocol traffic to relearn working, loop-free routes on mobile networks of wide diameter.

The majority of routing protocols, which are non-loop-free under dynamic topologies, exhibit transient looping behavior after topology changes. The inner face behavior is transient in this way: once the inner face forms, it only traps packets inside it, and subsequent packets between the same source and destination pair will be forwarded without looping. An adversary can always move nodes so as to provoke looping behavior by these protocols, and can do so in GPSR by endlessly creating new inner faces.

Synthesizing the above, we take the view that perimeters are a *recovery mechanism* for greedy forwarding. They allow greedy forwarding to reach 100% of connected destinations on static networks, and improve the robustness of greedy forwarding on mobile networks, as well. The classic challenges for routing protocols are routing on dynamic topologies, topologies with numerous nodes, or topologies with both these characteristics. GPSR has been shown to scale well on dense, large-scale mobile networks and on sparser mobile networks. It also will scale well on relatively static topologies with large numbers of nodes (*e.g.*, rooftop networks [37]), where pushing global state, even infrequently, is prohibitively expensive because of the number of destinations in the network.

We expect that for any fixed node density, as the diameter of the network increases, there exists a threshold diameter beyond which GPSR will deliver a greater fraction of packets successfully than DSR. The measurements in Section 4.5 show this trend on dense

networks. On sparser networks, GPSR will use perimeters more frequently. Perimeter-mode forwarding is less robust than greedy-mode forwarding under mobility. Starting from a 50-node sparse network of the type simulated in Section 4.6, let us build a wider-diameter network of equal density, by tiling several such 50-node sparse networks adjacent to each other, in an n -tile-by- n -tile grid. The average end-to-end route length in the wider-diameter network increases with n . And the frequency with which a DSR source route breaks on average will also increase with n . Thus, as network diameter increases, under mobility, the routes learned by a source node under DSR will be valid for progressively shorter intervals, and in the limit, a DSR source will not succeed in learning routes that are still valid by the time they return, if they return at all. In contrast, GPSR does not use end-to-end state in forwarding. Thus, the chance that GPSR succeeds in forwarding a packet at each hop, whether in greedy mode or perimeter mode, depends only on the local topology, which depends on the density of nodes and mobility rate, and not the network diameter. On average, GPSR should succeed in routing a packet across each of the n^2 tiles with equal probability. This argument suggests that GPSR will offer lower delivery success rates as network diameter increases, as is borne out in the results in Chapter 4. In summary, each GPSR forwarding decision uses only local state, whose accuracy is *independent of network diameter*, while DSR uses end-to-end state, whose accuracy *depends on network diameter*.

5.2 System Design for GPSR Networks

The addition of location registration and lookup traffic for a location database will increase GPSR's overhead. For bidirectional traffic flows between end nodes, a location database

lookup will often need only be performed by the connection initiator at the start of a connection; thereafter, both connection endpoints keep one another apprised of their changing locations by stamping their current locations in each data packet they transmit. In this case, the actual location database lookup is a one-time, DNS-like lookup.

It is important to note that GPSR decouples participation in routing as a forwarder from participation in the location database. Only nodes that are traffic destinations need send location updates to the database, and only nodes that originate traffic need send location queries to it. In a dense sensor network [19], it is easy to imagine configuring only a small subset of sensor nodes to take measurements at only the current points of interest, by flooding a few configuration packets through the network. The remainder of the sensor network can provide a robust transit network for the collection of measurements from sensors to the measurement point, with GPSR's beacons as their only routing protocol traffic—*without* generating any traffic to and from the location database.

In some networks, a destination may inherently have a well-known location. For example, the position of one or more fixed data collection points for a sensor network may be known to all sensors, in which case no location database is needed.

It is also important to note that queries and registrations for the location database are routable using GPSR itself; the queries and registrations are geographically addressed. GRID [25] is an instance of just such a location database system, whose packets are all generated with native geographical addresses.

Storing nodes' velocity vector information in the location database, besides their instantaneous positions, would allow extrapolation of nodes' positions without additional

queries to the location database. This technique is promising because the predictability of an object's motion tends to be correlated with the object's velocity (*e.g.*, passenger jets, automobiles on Interstate highways), though there are of course exceptions, such as military fighter jets.

5.3 Future Work

One assumption in the use of planar perimeters we would like to investigate further is that a node can reach all other nodes within its radio range. The GG and RNG planarizations both rely on a node's ability to accurately know if there is a witness w within radio range, when considering elimination of an edge to a known neighbor. Our use of the GG and RNG can disconnect a graph with particular patterns of obstacles between nodes. This disconnection is easily avoided by forcing the pair of nodes bordering an edge to agree on the edge's fate, with two rules:

- Both nodes must decide to eliminate the edge, or neither will do so.
- If both nodes decide to eliminate the edge, they must agree on a common w (*i.e.*, there must be a transitive path through a witness they can *both* reach).

However, this modification to the planarization algorithms will make the RNG and GG planarizations leave one or more crossing edges in these regions with obstacles. We intend to study these cases further. One promising approach in dealing with such obstacles may be to have obstructed nodes choose a reachable *partner* node elsewhere in the network, and route via the partner for destinations that are unreachable because of local failure of

the planarization. One engineering choice that can assist in avoiding difficulties caused by barriers to radio propagation is to choose a conservative threshold distance for the radios, and to ignore links to neighbors who are reachable but located beyond this threshold. Such a choice allows one to deploy nodes more densely to engineer away barriers to radio propagation. For example, 900 MHz battery-powered radios, such as Metricom Ricochet radios, which transmit at 1 W, propagate their signal so well indoors that a single radio on the top floor of a large building can reach other radios at any point in the building. Thus, it is possible to build radios where barriers such as multiple walls and floors still allow a reasonable conservative threshold distance under which connectivity is assured.

Hybridizing GPSR with Distance-Vector routing may both improve GPSR's robustness in the presence of obstacles, and allow GPSR to recover from imprecision in the destination location stamped in a packet, caused by the continuing motion of the destination between the time it reported its location to the location database and when a packet is forwarded using that imprecise location. First, we note that the beaconing protocol conducted by GPSR *is* a kind of Distance-Vector routing, where the propagation of nodes' information is limited to a single hop. A k -hop Distance-Vector protocol propagates nodes' position and transitive reachability information for k hops. Increasing k in GPSR's beaconing protocol would provide information to nodes about the entire set of reachable destinations within k hops of them. Obstacles are most often local phenomena. Localized shortest-path (k -hop DV) routing would assist nodes in forwarding around local obstacles *without* using perimeters. Moreover, a packet only needs to reach a node within k hops of the destination's current position to be forwarded successfully to the destination. So increasing k would

increase GPSR's tolerance for imprecision in packets' destination location fields. Of course increasing k will increase GPSR's routing protocol overhead, both because the number of nodes mentioned in a beacon packet will increase, and because more frequent beacons will be necessary to keep consistent topological state at all nodes.

While we have shown herein the benefits of geography as a tool for scalable routing systems, measuring the combined behavior of GPSR and a location database system will reveal more about the costs of using geography for routing. An efficient distributed location database would provide a network service useful in many other location-aware computing applications.

A comparison of the behavior of GPSR using the RNG and GG planarizations would reveal the performance effects of the tradeoff between the greater traffic concentration that occurs in perimeter forwarding on the sparser RNG, *vs.* the increased spatial diversity that the RNG offers by virtue of its sparsity. Even outside the context of GPSR, it may be the case that limiting edges used for forwarding in a radio network to those on the RNG or GG may reduce contention and improve efficiency on MAC protocols sensitive to the number of sending stations in mutual range.

Provisioning of bandwidth for geographically routed networks is an open problem. On wired networks, low capacity links exist at the edges of the network, which aggregate into higher capacity links, and so on; capacity is provisioned hierarchically, and hierarchical routing (BGP over an intra-domain routing protocol) matches the hierarchical capacity. On a naive rooftop network in a metropolitan area, where all radios have equal capacity, "hot spots" of traffic concentration can cause congestion. These hot spots will occur when con-

nections are geographically routed through the same region. We believe that geographic routing is naturally suited to a new kind of traffic provisioning that is not hierarchical, but geographic. Specifically, at flow setup time between a source and destination, a random geographic waypoint (or set of waypoints) can be chosen, and the flow forced to traverse those waypoint(s). The effect of such a scheme would be to spread the traffic spatially across the network. Routes would become non-shortest-path, but that effect exists in today's hierarchically provisioned networks. In fact, the operational definition of provisioning is elevation of capacity's importance above hop count's in making routing decisions. The fundamental reason that this scheme can work is that on a wireless network, *capacity is correlated with geography*, since spatial diversity increases capacity.

Hierarchy, useful in improving the scalability of wired Internet routing systems, should enhance GPSR's scalability as well, in networks where there are static boundaries for routing sub-domains. In networks whose nodes have heterogeneous radio ranges, and which are therefore not unit graphs, GPSR may not be able to make use of the longest links. A campus comprised of intra-campus links up to 250 m in length may have a 2 km point-to-point link to another site that terminates in the center of the local campus. If the entire network is a single geographic routing domain, nodes located between the center of the local campus and the remote site will forward greedily toward the boundary of the local campus, and the path to the remote site from this boundary will not consist of faces that are progressively closer to the destination, as is the case in networks that are unit graphs. Hierarchy can salvage this situation: nodes inside the local campus can geographically route packets destined for outside the campus to position of the campus gateway. Intra-campus

links comprise a unit graph with one threshold, and inter-campus links comprise a separate unit graph, the upper level in the hierarchy, with a greater threshold. Finn [10] touches on the potential utility of hierarchy in greedy geographic routing.

We hope to extend GPSR for hosts placed in three-dimensional space, beyond the flat topologies explored in this thesis. Greedy forwarding extends simply to three dimensions. However, a three-dimensional analog for planar perimeter forwarding is harder to achieve. A promising approach is to implement perimeter forwarding for 3-D *volumes* rather than 2-D faces. There exists an algorithm for computing the Relative Neighborhood Graph for a set of points placed in three dimensions [40] (the result is a graph in which no plane cutting the 3-D space contains two crossing edges—a lattice-like structure). However, this algorithm is not distributed in the way the two-dimensional one is; it requires the entire topology be known to a single entity computing the RNG. Traversing the surfaces of these volumes will be more akin to search than to the straightforward, cycle-traversing right-hand rule.

Chapter 6

Related Work

Finn [10] is the earliest we know to propose greedy routing using the locations of nodes. He recognizes the small forwarding state greedy forwarding requires, and observes the failure of greedy forwarding upon reaching a local maximum. He proposes flooding search for a closer node as a strategy for recovering from local maxima.

We first propose greedy forwarding and perimeter traversal in [22], as briefly discussed in Section 3.1. This work simulates this older algorithm on static networks, in a very idealized (contentionless, infinite bandwidth) simulator, and presents the state per node (including perimeter node lists, notably absent from the current work), message cost from cold start to convergence, and frequency with which routes are not found, because of the imperfect no-crossing heuristic. This prior work does not offer any mobile simulation results, and the earlier algorithm suffers in many ways from its maintenance of state beyond neighbor lists at all routers: increased state size for perimeter lists at all nodes, periodic pro-active routing protocol traffic that perimeter probes generate, and staleness of prime-

ter lists that would occur under mobility. The unreachability of even a small fraction of destinations on *static* networks because of the failure of the no-crossing heuristic is also problematic; such routing failures are permanent, not transitory.

Johnson and Maltz [18] propose the Dynamic Source Routing (DSR) protocol. DSR generates routing traffic reactively: a router floods a route request packet throughout the network. When the request reaches the destination, the destination returns a route reply to the request's originator. Nodes aggressively cache routes that they learn, so that intermediate nodes between a querier and destination may subsequently reply on behalf of the destination, and limit the propagation of requests. More recently, Hu and Johnson [16] evaluate a variety of caching schemes for DSR under several mobility models, and present measurements of their relative performance taken on 50-node networks.

Broch *et al.* [7] compare the performance of the DSDV, TORA, DSR, and AODV routing protocols on a simulated mobile IEEE 802.11 network. They simulate networks of 50 nodes, under a range of mobility rates and traffic loads. Their measurements show the effectiveness of DSR's caching in minimizing DSR's routing protocol traffic on these 50-node networks. DSR and AODV deliver by far more packets successfully with by far less routing protocol overhead than the other algorithms measured when mobility is most rapid. In the interest of comparability of results, we use this work's ns simulation environment for IEEE 802.11, a two-ray ground reflection model, and DSR.

Ko and Vaidya [24] describe Location Aided Routing (LAR), an optimization to DSR in which nodes limit the propagation of route request packets to the geographic region where it is most probable the destination is located. LAR uses base DSR to establish first

connectivity with a destination; thereafter, a route querier learns the destination's location directly from the destination node, and uses this information to mark route requests for propagation only within a region of some size about the destination's last known position. Like DSR's caching, LAR is a strategy for limiting the propagation of route requests. When a circuitous path, outside the region LAR limits route request propagation within, becomes the only path to a destination, LAR reverts to DSR's flooding-with-caching base case. Under LAR, DSR's routes are still end-to-end source routes. Geography is not used for data packet forwarding decisions under LAR; only to scope routing protocol packet propagation.

Basagni *et al.* [2] present DREAM, an integrated location dissemination and geographic routing system. In DREAM, all nodes store a location table mapping every node's address to its position. Every node originates position reports periodically, at a rate proportional to its own mobility rate. Position reports are flooded, but they are propagated varying distances. Nodes originate position reports most frequently with short distance propagation limits, and most rarely with long (*i.e.*, network-wide) propagation limits. In this regime, the precision of a location table entry for a destination is greatest in nodes near that destination, and progressively less in nodes increasingly farther away. This strategy avoids flooding position reports network-wide as frequently as a naive flooding protocol, and exploits the fact that the direction of the destination is less sensitive to error in the destination's position, the farther one is from the destination. Packets are marked only with the destination's address. To forward a packet, a node looks up the location of the destination in its local location table, and forwards the packet to all its neighbors in the direction of the destination,

where “in the direction of” is defined as within an arc centered on the destination. DREAM uses the estimated movement rate of the destination to bound the destination’s position within a circular region. The arc inside which the packet is forwarded is bounded by the two lines from the forwarding node that are tangent to this circle about the destination. When the forwarding node has no neighbors within this arc, it drops the packet. DREAM forces all packets to be sent reliably by their originator, and the originator falls back on flooding (or other techniques, unspecified by Basagni *et al.*) to discover a route to the destination when no acknowledgement returns for a packet. DREAM can deliver exponentially many copies of a packet to the destination; at each hop, the packet is forwarded to *all* neighbors within the arc in the appropriate direction, and those duplicates are in turn duplicated at subsequent hops. The authors argue that this packet duplication is a robustness feature, but it is unnecessarily wasteful of the network’s capacity. Lin and Stojmenović [26] present an example in which DREAM will loop traffic, even on a *static* network, assuming a relatively large forwarding arc. However, because the choice of arc when the destination has a *fixed* position is not explained in [2], this example may or may not be relevant.¹

Li *et al.* [25] propose GLS, a scalable and robust location database that geographically addresses queries and registrations. Their system dynamically selects multiple database servers to store each node’s location, for robustness against server failure. This property also ensures that a cluster of nodes partitioned from the remainder of the network continues to have location database service, provided by nodes inside the cluster. GLS uses a geographic hierarchy to serve queries at a server topologically close to the querier. The sys-

¹As specified in [2], one would expect the arc to be zero degrees when the position of the destination is fixed. But this would mean the forwarder would forward only to nodes exactly *on* the line to the destination.

tem spreads the work of the location database evenly across all nodes, by using *Consistent Hashing* [20] to induce separate caching hierarchies for each node's position information.

Bose *et al.* [5] independently investigated the graph algorithms for rendering a radio network's graph planar. They suggest the Gabriel Graph, and analyze the increase in path length over shortest paths when traversing a graph using *only* perimeters. Motivated by the longer-than-optimal paths perimeter traversal alone finds, they suggest combining planar graph traversal with greedy forwarding, and verify that this combination produces path lengths closer to true shortest paths. They present these algorithms at an abstract level. They do not present a routing protocol, do not simulate a network at the packet level, and assume that all nodes are stationary and reachable. In a revised version of this work [6], Bose *et al.* state that the extension of their static graph traversal algorithms to dynamic, changing networks is an open problem, and that they are unsure of how to evaluate the mobile versions of their algorithms in simulation.

Chapter 7

Conclusion

We have presented Greedy Perimeter Stateless Routing, GPSR, a routing algorithm that uses geography to achieve small per-node routing state, small routing protocol message complexity, and extremely robust packet delivery on densely deployed wireless networks. GPSR forwards greedily where topology allows, and benefits from the robustness and tendency toward shortest paths of greedy forwarding. Where greedy forwarding is impossible, GPSR uses perimeter forwarding to recover, and reach a region of the network where greedy forwarding can resume. Perimeter forwarding diverges from shortest paths, and is sometimes transitorily less robust for packets in mid-traversal on a perimeter that changes. GPSR scales well as the number of nodes and mobility rate increase. Our simulations on dense mobile networks with up to 200 nodes over a full IEEE 802.11 MAC demonstrate GPSR's scalability: GPSR consistently delivers upwards of 94% of data packets successfully; it is competitive with DSR in this respect on 50-node networks at all pause times, and increasingly more successful than DSR as the number of nodes increases, as demon-

strated on 112-node and 200-node networks. GPSR generates routing protocol traffic in a quantity independent of the length of the routes through the network, and therefore generates a constant, low volume of routing protocol messages as mobility increases, yet doesn't suffer from decreased robustness in finding routes. DSR must query longer routes as the network diameter increases, and must do so more often as mobility increases, and caching becomes less effective. Thus, DSR generates drastically more routing protocol traffic in our 200-node and 112-node simulations than it does in our 50-node ones. Finally, GPSR keeps state proportional to the number of its neighbors, while both traffic sources and intermediate DSR routers cache state proportional to the product of the number of routes learned and route length in hops.

We note that DSR by design does not make use of geographic information. This point, while far from subtle, is worth mentioning explicitly because GPSR benefits greatly from using information beyond that available to DSR.

In this thesis, we contribute:

- An architectural description of geographic forwarding as a scaling strategy for routing, and its relationship to hierarchy and caching, two other routing scaling strategies.
- A description of application areas where routing faces scaling challenges in number of nodes and rate of motion of nodes.
- The application of planar graphs to routing for wireless networks, to allow recovery from greedy forwarding failure on all static networks.
- The GPSR routing algorithm, which performs all forwarding decisions at a node

using *only* information concerning that node's immediate, single-hop neighbors.

- The full, dynamic GPSR routing protocol, designed for robustness on mobile networks, including integration with feedback from the MAC layer, dynamic triggering of the planarization algorithm, and support for detecting and dropping packets for disconnected destinations.
- A detailed, simulation-based performance evaluation of the GPSR and DSR mobile routing protocols on mobile networks, that shows GPSR scales well in increasing number of nodes and mobility by keeping small state, and shows that DSR-style source routing with caching does not scale, because caching's effectiveness declines with mobility and network diameter.

GPSR's benefits all stem from geographic routing's use of only immediate-neighbor information in forwarding decisions. Routing protocols that rely on end-to-end state concerning the path between a forwarding router and a packet's destination, as do source-routed, DV, and LS algorithms, face a scaling challenge as network diameter in hops and mobility increase because the product of these two factors determines the rate that end-to-end paths change. Hierarchy and caching have proven successful in scaling these algorithms. Geography, as exemplified in GPSR, represents another powerful lever for scaling routing.

Bibliography

- [1] ABRAMSON, N. The ALOHA system - another alternative for computer communications. *AFIPS 37* (1970), 281–285.
- [2] BASAGNI, S., CHLAMTAC, I., SYROTIUK, V., AND WOODWARD, B. A distance routing effect algorithm for mobility (DREAM). In *Proceedings of the Fourth Annual ACM/IEEE International Conference on Mobile Computing and Networking (MobiCom '98)* (Dallas, Texas, USA, Aug. 1998), pp. 76–84.
- [3] BETTENDORFF, J. Personal communication. Metricom, Inc., Sept. 1997.
- [4] BHARGHAVAN, A., DEMERS, S., SHENKER, S., AND ZHANG, L. MACAW: A media access protocol for wireless LANs. In *Proceedings of the SIGCOMM '94 Conference on Communications, Architectures, Protocols, and Applications* (Sept. 1994), pp. 212–225.
- [5] BOSE, P., MORIN, P., STOJMENOVIĆ, I., AND URRUTIA, J. Routing with guaranteed delivery in *ad hoc* wireless networks. Workshop on Discrete Algorithms and Methods for Mobile Computing and Communications (DialM '99), Aug. 1999.

- [6] BOSE, P., MORIN, P., STOJMENOVIĆ, I., AND URRUTIA, J. Routing with guaranteed delivery in *ad hoc* wireless networks. <http://www.site.uottawa.ca/ivan/unitgraphs.ps>, Dec. 1999.
- [7] BROCH, J., MALTZ, D., JOHNSON, D., HU, Y., , AND JETCHEVA, J. A performance comparison of multi-hop wireless ad hoc network routing protocols. In *Proceedings of the Fourth Annual ACM/IEEE International Conference on Mobile Computing and Networking (MobiCom '98)* (Dallas, Texas, USA, Aug. 1998).
- [8] CALI, F., CONTI, M., AND GREGORI, E. IEEE 802.11 wireless LAN: capacity analysis and protocol enhancement. In *Proceedings of IEEE INFOCOM 1998* (San Francisco, California, March/April 1998), p. 142.
- [9] CHANDRAKASAN, A., AMIRTHARAJAH, R., CHO, S., GOODMAN, J., KONDURI, G., KULIK, J., RABINER, W., AND WANG, A. Design considerations for distributed microsensor systems. In *Proceedings of the IEEE 1999 Custom Integrated Circuits Conference (CICC '99)* (May 1999), pp. 279–286.
- [10] FINN, G. G. Routing and addressing problems in large metropolitan-scale internet-works. Tech. Rep. ISI/RR-87-180, Information Sciences Institute, Mar. 1987.
- [11] FLOYD, S., AND JACOBSON, V. The synchronization of periodic routing messages. *IEEE/ACM Transactions on Networking* 2, 2 (April 1994), 122–136.
- [12] GABRIEL, K., AND SOKAL, R. A new statistical approach to geographic variation analysis. *Systematic Zoology* 18 (1969), 259–278.

- [13] HAAS, Z., AND PEARLMAN, M. The performance of query control schemes for the zone routing protocol. In *Proceedings of the SIGCOMM '98 Conference on Communications Architectures, Protocols and Applications* (Sept. 1998).
- [14] HEDRICK, C. E. Routing information protocol. Internet Request for Comments RFC 1058, June 1988.
- [15] HOU, T., AND LI, V. Performance analysis of routing strategies in multihop packet radio networks. In *Proceedings of IEEE GLOBECOM 1984* (1984), pp. 487–492.
- [16] HU, Y., AND JOHNSON, D. Caching strategies in on-demand routing protocols for wireless ad hoc networks. In *Proceedings of the Sixth Annual ACM/IEEE International Conference on Mobile Computing and Networking (MobiCom 2000)* (Boston, Massachusetts, USA, Aug. 2000).
- [17] IEEE COMPUTER SOCIETY LAN MAN STANDARDS COMMITTEE. Wireless LAN Medium Access Control (MAC) and Physical Layer (PHY) Specifications. IEEE Std. 802.11-1997, 1997.
- [18] JOHNSON, D. B., AND MALTZ, D. B. Dynamic source routing in ad hoc wireless networks. In *Mobile Computing*, T. Imielinski and H. Korth, Eds. Kluwer Academic Publishers, 1996, ch. 5, pp. 153–181.
- [19] KAHN, J. M., KATZ, R. H., AND PISTER, K. S. J. Mobile networking for smart dust. In *Proceedings of the Fifth Annual ACM/IEEE International Conference on Mobile Computing and Networking (MobiCom '99)* (Seattle, WA, USA, Aug. 1999).

- [20] KARGER, D., LEHMAN, E., LEIGHTON, T., LEVINE, M., LEWIN, D., AND PANIGRAHY, R. Consistent hashing and random trees: Distributed caching protocols for relieving hot spots on the world wide web. In *Proceedings of the 29th ACM Symposium on Theory of Computing* (May 1997), pp. 654–663.
- [21] KARN, P. MACA—a new channel access method for packet radio. In *Proceedings of the 9th Computer Networking Conference* (Sept. 1990), pp. 134–140.
- [22] KARP, B. Greedy perimeter state routing. Invited Seminar at the USC/Information Sciences Institute, July 1998.
- [23] KARP, B., AND KUNG, H. GPSR: greedy perimeter stateless routing for wireless networks. In *Proceedings of the Sixth Annual ACM/IEEE International Conference on Mobile Computing and Networking (MobiCom 2000)* (Boston, Massachusetts, USA, Aug. 2000).
- [24] KO, Y., AND VAIDYA, N. Location-aided routing in mobile ad hoc networks. In *Proceedings of the Fourth Annual ACM/IEEE International Conference on Mobile Computing and Networking (MobiCom '98)* (Dallas, Texas, USA, Aug. 1998).
- [25] LI, J., JANNOTTI, J., DECOUTO, D., KARGER, D., AND MORRIS, R. A scalable location service for geographic ad-hoc routing. In *Proceedings of the Sixth Annual ACM/IEEE International Conference on Mobile Computing and Networking (MobiCom 2000)* (Boston, MA, USA, Aug. 2000).
- [26] LIN, X., AND STOJMENOVIĆ, I. Gps-based routing algorithms for wireless networks. Tech. Rep. TR-98-10, SITE, University of Ottawa, Dec. 1998.

- [27] MALTZ, D., BROCH, J., JETCHEVA, J., AND JOHNSON, D. The effects of on-demand behavior in routing protocols for multihop wireless ad hoc networks. *IEEE Journal on Selected Areas in Communications* 17, 8 (Aug. 1999), 1439–1453.
- [28] MCQUILLAN, J. M., RICHER, I., AND ROSEN, C. The new routing algorithm for the ARPANET. *IEEE Transactions on Communications* 28, 5 (1980), 711–719.
- [29] MORRIS, R., JANNOTTI, J., KAASHOEK, F., LI, J., AND DECOUTO, D. Carnet: A scalable ad hoc wireless network system. The 9th ACM SIGOPS European Workshop: Beyond the PC, New Challenges for the Operating System, Sept. 2000.
- [30] MORRIS, R., AND KARP, B. Greedy perimeter state routing. Draft (submitted to MobiCom 1998; rejected), Apr. 1998.
- [31] NELSON, R., AND KLEINROCK, L. The spatial capacity of a slotted aloha multihop packet radio network with capture. *IEEE Transactions on Communications* 32, 6 (June 1984), 684–694.
- [32] PARK, V., AND CORSON, M. A highly adaptive distributed routing algorithm for mobile wireless networks. In *Proceedings of the Conference on Computer Communications (IEEE Infocom)* (Kobe, Japan, Apr. 1997), pp. 1405–1413.
- [33] PERKINS, C. Ad hoc on demand distance vector (AODV) routing. Internet-Draft, draft-ietf-manet-aodv-04.txt, Oct. 1999.
- [34] PERKINS, C., AND BHAGWAT, P. Highly-dynamic destination-sequenced distance-vector routing (DSDV) for mobile computers. In *Proceedings of the SIGCOMM '94*

- Conference on Communications, Architectures, Protocols, and Applications* (London, UK, Sept. 1994), pp. 234–244.
- [35] PRIYANTHA, N., CHAKRABORTY, A., AND BALAKRISHNAN, H. The cricket location-support system. In *Proceedings of the Sixth Annual ACM/IEEE International Conference on Mobile Computing and Networking (MobiCom 2000)* (Boston, Massachusetts, USA, Aug. 2000).
- [36] SALTZER, J., REED, D. P., AND CLARK, D. End-to-end arguments in system design. *ACM Transactions on Computer Systems* 2, 4 (Nov. 1984), 277–288.
- [37] SHEPARD, T. A channel access scheme for large dense packet radio networks. In *Proceedings of the SIGCOMM '96 Conference on Communications Architectures, Protocols and Applications* (Aug. 1996).
- [38] THE CMU MONARCH GROUP. Wireless and Mobility Extensions to ns-2. <http://www.monarch.cs.cmu.edu/cmu-ns.html>, Oct. 1999.
- [39] THE VINT PROJECT. The UCB/LBNL/VINT Network Simulator—ns (version 2). <http://mash.cs.berkeley.edu/ns>.
- [40] TOUSSAINT, G. The relative neighborhood graph of a finite planar set,. *Pattern Recognition* 12, 4 (1980), 261–268.
- [41] WARD, A., JONES, A., AND HOPPER, A. A new location technique for the active office. *IEEE Personal Communications* 4, 5 (Oct. 1997), 42–47.

- [42] ZAUMEN, W., AND GARCIA-LUNA ACEVES, J. Dynamics of distributed shortest-path routing algorithms. In *Proceedings of the SIGCOMM '91 Conference on Communications Architectures, Protocols and Applications* (Sept. 1991), pp. 31–42.